NASA CONTRACTOR REPORT

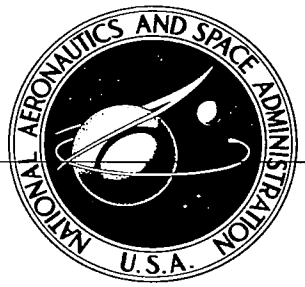


NASA CR-535

c. 1

NASA CR-534



# FLIGHT TYPE OXYGEN PARTIAL PRESSURE SENSOR

*by S. A. Sternbergh and W. M. Hickam*

*Prepared by*
WESTINGHOUSE ELECTRIC CORPORATION
Pittsburgh, Pa.
*for Langley Research Center*

NATIONAL AERONAUTICS AND SPACE ADMINISTRATION • WASHINGTON, D. C. • AUGUST 1966

NASA CR-534

# FLIGHT TYPE OXYGEN PARTIAL PRESSURE SENSOR

By S. A. Sternbergh and W. M. Hickam



Prepared under Contract No. NAS 1-4340 by
WESTINGHOUSE ELECTRIC CORPORATION
Pittsburgh, Pa.

for Langley Research Center

NATIONAL AERONAUTICS AND SPACE ADMINISTRATION

For sale by the Clearinghouse for Federal Scientific and Technical Information
Springfield, Virginia 22151 – Price $2.00

## TABLE OF CONTENTS

# FLIGHT TYPE OXYGEN PARTIAL PRESSURE SENSOR

## I. SUMMARY

A miniature, flight type, oxygen sensor has been developed by Westinghouse Scientific Equipment Department which uses a high temperature solid electrolyte as the sensing element, or cell. The electrolyte is calcium stabilized zirconium oxide. The cell is a double bore tube in which the walls of each bore are coated with porous platinum films which act as electrodes. Platinum capillary tubes are attached to the sensor openings to direct the entering and exiting gases, to provide for heat exchange between these gases, and to provide contacts to the electrodes. An electrical heater coil, wound on a ceramic tube, is positioned around a portion of the cell to provide for heating the cell to its operating temperature of 850°C. The entire assembly is insulated to reduce the heating load.

This electrochemical cell provides a signal voltage which is proportional to the logarithm of the ratio of the partial pressures of oxygen at the two electrodes. The output signal voltage is described by the Nernst equation:

$$E = \frac{RT}{nF} \ln \frac{P_1\ (O_2)}{P_2\ (O_2)} \qquad \text{Equation 1}$$

where R is the gas constant, T is the temperature, °K, n is taken as 4 from the reversible reaction $O_2 + 4e \rightleftharpoons 2\ O^{=}$, F is the Faraday constant, and $P_1\ (O_2)$ and $P_2\ (O_2)$ are the partial pressures of oxygen at the two electrodes.

The sensor weighs about fifty grams, occupies 18cc of volume and uses 14 watts of d-c power. The reference and test gases flow at rates of .06 SCFH or less at atmospheric pressures.

The sensor is not dependent on gravimetric forces and is suitable for flight applications. It is insensitive to water, carbon dioxide and nitrogen which are commonly found in atmospheres supporting life.

In the range of partial pressures of oxygen from 100 mm to 200 mm Hg the sensor has demonstrated, in limited tests, its ability to measure oxygen levels within 2% of the amount of oxygen present.

The dual flow configuration used has materially reduced the sensitivity of the cell to gas flow rates.

## II. ABSTRACT

A high temperature galvanic cell made of calcium stabilized zirconium oxide electrolyte with porous metallic electrodes was investigated as a means of continuously monitoring oxygen pressure in space capsules. These cells generate a voltage between their electrodes which is proportional to the logarithm of the ratio of the partial pressures of oxygen at the two electrodes. The current carrier through the solid electrolyte is ionic oxygen ($O^{=}$).

A miniature, flight type, oxygen sensor was developed which utilizes the high temperature galvanic cell and in which complete control of both the reference and test gases is possible.

A description of the oxygen pressure is given and test results of a prototype sensor are presented, along with life test data on Westinghouse standard cells operating under various conditions.

## III. INTRODUCTION

The life support systems in space capsules are directly concerned with maintaining a prescribed level of oxygen in the capsule ambient which will properly support life and in providing a continuous signal denoting this level. This report describes an oxygen sensor which can measure the oxygen level in a life support atmosphere and provide a continuous signal which can be used for controlling this level. The operation of the sensor is not dependent on gravimetric forces and is suitable for the intended use.

Any galvanic cell in which the electrode reactions involve oxygen can, in principle, be used to measure oxygen partial pressures. In the ideal and simplest case we have what is called an oxygen concentration cell, which is illus-

trated diagrammatically below:

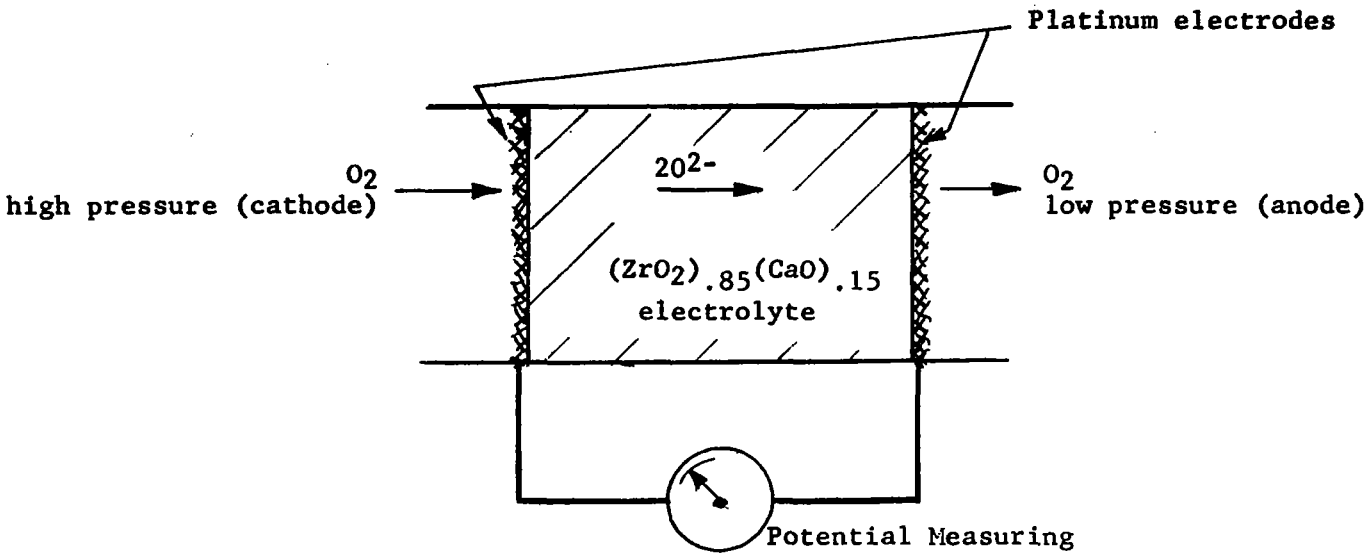


Schematic of Oxygen Concentration Cell

In this cell the following reactions take place at the electrode-electrolyte interfaces:

$$\text{Cathode:}\quad O_2 + 4e \rightleftharpoons 2\,O^{=}$$
$$\text{Anode:}\quad 2\,O^{=} \rightleftharpoons O_2 + 4e \qquad \text{Equation 2}$$

At the cathode oxygen enters the electrolyte as oxygen ions. Simultaneously, at the anode, oxygen molecules are reformed by the reverse action.

The voltage E of this galvanic cell is related to the oxygen partial pressures at the electrodes by the standard Nernst relationship for an oxygen concentration cell, Equation 1.

For the sensors to be described in this report the equation for the open circuit signal voltage E, in millivolts, reduces to:

$$E = .0496\ T \log_{10} \frac{P_1\ (O_2)}{P_2\ (O_2)}$$

for those cells operating at 850°C the voltage E, in millivolts, is:

$$E = 55.7 \log_{10} \frac{P_1\ (O_2)}{P_2\ (O_2)}$$

In order for the cell to provide reproducible output voltages over extended periods of time, it is essential to prevent "poisoning" of the electrodes. This can be accomplished either by replacing the cell periodically as required or by operating at a temperature which will provide for the automatic removal of "poison" contaminants (850°C). The latter method has been adopted since it is most practical and also provides for a suitably low resistance to ionic conduction to eliminate the need for sensitive amplification of the output signal.

In order to operate at this high temperature, materials must be selected which have both suitable temperature stability, good ionic conduction properties and high electrical impedance. Such a material is zirconia doped with calcium oxide which provides stable crystallographic stability and suitable ionic conductivity.

The conductivity in this material results from the presence of highly mobile vacancies at oxygen ion sites in the crystal lattice. One such vacancy exists for each $Ca^{2+}$ ion in the lattice. The conductivity is due nearly exclusively to oxygen ion or vacancy migration. Since electronic and metal ion conduction are virtually non-existent we have an ideal material for such applications.

If electronic conduction were present the cell emf would be lowered while metal ion conduction would result in transfer of solid materials of the electrolyte and/or electrodes which would adversely alter the electrode-electrolyte interfaces.

## IV. APPARATUS

### A. Standard Sensor

The solid electrolyte of the sensor electrochemical cells is a calcium stabilized zirconium oxide. The configuration of the standard cell is a single bore tube with porous platinum coatings applied to provide both an interior and an exterior electrode. The electrodes are applied as a thin platinum paste which is fired in air to burn off the organic vehicle. In small bores the rate of heating must be very slow to prevent blistering. Several coats were applied to obtain a suitable ohmic resistance of the electrodes and to provide good adherence.

The cell is heated over a portion of its length by an electrical heater wound on a ceramic tube which is positioned around a portion of the cell. Atmospheric air in contact with the external electrode is used as a reference oxygen partial pressure while test gas, flowing through the tube, will provide the second oxygen partial pressure necessary to generate an output signal. Contacts from the two cell electrodes are connected to a high impedance voltmeter for monitoring the output signal. In Figure 1 is shown a model of the Westinghouse line of standard oxygen gauges. Figure 2 shows a test set-up for standard size oxygen sensors which was used to run the life tests described in this report.

B. Miniature Sensor

The configuration of the miniature, flight type, cell is a double bore tube with porous platinum coatings applied to each of the parallel bores. The coating in one bore is broken at a point a short distance in from one end, while that of the second bore is broken similarly but at the opposite end. A platinum capillary tube is attached to each of the four openings of the cell, providing gas tight seals. Figure 3 shows the miniature cells, with gas capillaries attached, which are used in the flight type oxygen sensor. Figure 4 is an end view of a cell showing the hermetic seals. The attachment of the capillary tubes was accomplished in the following manner. The platinum tube ends were first individually fitted to the openings in the cell so that a minimum of radial clearance existed but without interference which could damage the platinum coatings in the bores as the tubes were inserted. The tips of the platinum tubes were then gold-plated in the vicinity of the proposed brazing area. The tubes were inserted into their bores and gold solder rings were placed around the tubes and in contact with the cell. They were then furnace heated to 1095°C. This provides a good electrical joint but not a hermetic seal. A glass frit was then placed around each joint and the unit was fired as before. The glass provides a hermetic seal. The tube attachment is made between the end of the cell and the breaks in the platinum coatings in the two bores so that the pair of platinum tubes emerging from one end of the cell are electrically isolated from the pair of tubes emerging from the opposite end of the cell.

These pairs of tubes will be the two contacts to the electrodes of the cell. As before, this cell is heated to operating temperature over a portion of its length by positioning an electrical heater wound on a ceramic tube around a portion of the cell. A thermocouple and a platinum resistance thermometer are

positioned within the heater ceramic tube and sense the temperature at points between the heater winding and the cell. A high temperature insulating cement is applied to the assembly to maintain the proper relative positions of the components, as shown in Figure 5. At this point the prototype sensor which was used to obtain test data for this report was potted in insulation and breadboarded as shown in Figure 6.

The final sensor design, however, provided for encapsulation of the device and the two pairs of platinum tubes were now shaped and brazed together throughout most of their length so that, with counterflow of the test and reference gases, they provide for the exchange of heat between the exiting and entering gases.

Iron-nickel-cobalt alloy tubes, prepared with glass-beaded sections, are brazed to each of the four platinum capillaries and the sensor is mounted on a vidicon tube press, as shown in Figure 7. You will note that the sensor is mounted rigidly to two long inner pins of the press to provide support against accelerations and shock. All electrical connections are made to the pins of the press except the thermocouple leads. These pass through holes prepared through two pins of the press. This is done to eliminate the error which a temperature drop along these pins would otherwise introduce. A glass envelope is sealed over this assembly, as shown in Figure 8. Insulation is packed inside the envelope to complete the sensor, as shown in Figure 9. The insulating material is fibrous potassium titanate which has excellent thermal properties at temperatures to 1200°C. The insulation provides additional support for the sensor against accelerations and shock.

The completed sensor has been mounted on a base to provide a miniaturized oxygen sensor system. Gas connections from any selected sources can be made

to 1/4" copper tubes mounted on the upstream side of two (2) three-way valves. These valves are used to quickly purge unwanted gases from the large volume gas lines and pressure regulators by venting the lines to atmosphere. After the purging is completed the valves are turned to direct the gases to the sensor through plastic capillary tubes. Figure 28 is a curve of flow rates through these capillaries versus gas pressures applied to the valve inlets. A terminal strip is mounted on the base for ease of applying heater power and monitoring temperatures with the thermocouple (T/C+ and T/C-) and the platinum resistance thermometer (TH). The vidicon tube receptacle must be applied per the drawing of the sensor assembly to insure the application of heater power to the correct sensor pins. Figure 10 is a photograph of the completed oxygen partial pressure sensor system.

## V. EXPERIMENTAL PROCEDURE AND DISCUSSION

### A. Standard Size Sensor

Test systems containing the standard solid electrolyte cell shown in Figure 2 were used in evaluating the performance of the electrolyte with various gas mixtures, variations due to flow rates, establish the current capacity of the cell when used for oxygen monitoring, to measure the temperature influence on its operation, and to carry out life tests. The standard gas mixture used in the tests was obtained from Air Products in standard 220 cu.ft. high pressure cylinders. The mixture contained specific concentrations of oxygen with the remainder nitrogen.

In Figure 11 is shown the cell output voltage versus flow curves obtained at 10 ppm, $1.32 \times 10^5$ ppm, and $2.64 \times 10^5$ ppm for 600°C, 750°C, and 850°C. The reference gas was ambient air. In the standard cell the difference in signal

between no flow and flow at 2 SCFH of the sample gas is of the order of 3 mv for identical gas compositions at both electrodes. In the mixtures that have less oxygen than air the magnitude of the signals decreases with increased flow. In the case of $2.64 \times 10^5$ ppm of oxygen the magnitude of the voltage signal increases with the increase of flow. The change in signal is associated with the increase in pressure required to bring about the flow through the cell. The shift in the voltage with temperature is in reasonable agreement with the temperature change (°K). The high resistance of the electrolyte at 600°C makes it difficult to work at this temperature. Differences from the theoretical shifts are believed due to errors in temperature measurements and non-uniformity of cell temperature rather than to represent a departure from the Nernst relationship.

The shape of the voltage versus current curves for 850°C and 600°C using two gas mixtures are given in Figure 12. The open circuit voltage is maintained for a current drain of the order of 100$\mu$a at 850°C. The higher resistance of the electrolyte at 600°C leads to sizable departures from the open circuit voltage at less than 1$\mu$a. If the cell was used at 600°C for monitoring, the signal monitoring equipment would be required to have an input impedance approximately one hundred (100) times that required for monitoring at 850°C operation.

Voltage versus oxygen concentration curves are given in Figure 13 for 600°C, 750°C and 850°C for the standard solid electrolyte sensor. The change in slope with temperature is in reasonable agreement with that calculated from the Nernst equation.

The standard sensor systems were assembled and connected through valves to cylinders containing 13.2% oxygen and 26.4% oxygen in nitrogen for life test. The cells were maintained at 850°C, 750°C and 650°C, respectively, during a 100-

day life test. Each Monday, Wednesday and Friday the gas samples were flowed through the cell at 4 SCFH and the output voltage measured. Figure 2 is a photograph of one of the units used in the life test. The results of the 100-day life tests are shown in Figures 14 and 15. The voltage output at 850°C is more stable than at either of the lower temperatures. A reduction in power requirement by lower operating temperatures does not appear attractive from the life test curves. The theoretical voltage for the 850°C curve of Figure 14 is 11.2 mv and for Figure 15 is 5.6 mv. The voltage displacement in the curves is in line with that illustrated in Figure 11.

In each case the measured voltage is 4-5 mv from the theoretical at 4 SCFH flowrate. The advantage of a dual flow system in compensating for this difference is obvious if precise results are required.

The variations in atmospheric pressure over the 100-day life tests were followed in order to see if any observed fluctuations in cell response could be correlated with this parameter. Figure 16 is a plot of recorded atmospheric pressure at the Research site during the test period at the time of measurement. The observed drift in the 650°C and 750°C curves of Figure 14 and Figure 15 are in the appropriate direction to correlate with changes in atmospheric pressures during this period. However, the magnitude of the voltage change is much too large to be explained by atmospheric pressure changes. Furthermore, the more reliable 850°C curves do not show this trend. Pressure in the laboratory room may not reflect the atmospheric pressure at the site due to forced air heating and cooling systems.

B. Six Inch Long Double Bore Sensor

In order to investigate the performance of a double bore cell of the same general design shown in Figure 3, test data was obtained on a double bore cell having a length of six (6) inches. The interior of the entire length of the holes was coated with platinum. A portion of the cell was heated and temporary room temperature seals made to each bore. Characteristic curves obtained on this six inch small double bore cell are given in Figure 17. The agreement of the curves at high oxygen concentration with the theoretical curves is satisfactory. The departure at low oxygen concentration is believed due to minute leaks and back diffusion of air.

C. Prototype Miniature Sensor

The data given in Figures 18-27 were obtained on the prototype miniature sensor system shown in Figure 6. The details of assembly of the sensor are shown in Figures 3, 4 and 5.

In Figure 18 is given the voltage versus oxygen concentration curves obtained at 600°C, 750°C and 850°C using .06 SCFH flow rates and a reference gas of 19.7% oxygen in nitrogen. The curves agree at high oxygen concentration reasonably well with those of Figure 17. The close agreement of the 1000 and 10 ppm voltage points suggests a leak in the system or back diffusion of air.

Voltage versus current curves for the miniature cell are shown in Figure 19 for an operating temperature of 850°C and gas flow rate of .06 SCFH through both inlets. This curve suggests that open circuit voltage is maintained up to a current of the order of $4 \times 10^{-7}$ amperes. Earlier data obtained showed that reasonable measurements could be made with current drains in the range of $1\text{-}5 \times 10^{-6}$ amperes. It is believed that with additional experience in electrode

coating of the miniature cell, open circuit voltages can be maintained for a current drain of $1 \times 10^{-6}$ amperes.

In order to establish the benefits derived from the use of a dual flow system as compared to the single flow system used in the standard cell, a large quantity of data was obtained for various flow conditions. Figures 20-22 are examples of curves obtained of the observed output voltage versus flow rates. The flow requirements have been reduced by about a factor of a hundred in going from the standard cell to the miniature cell. The variations in output voltage with flow have been greatly reduced in going to the dual flow system. In fact, it is difficult to correlate the changes observed in a number of the curves of Figures 20-22 as being due to flow and suggest that other factors may be contributing to the observed voltage changes.

In order to obtain information on the magnitude of voltage changes independent of flow, drift curves such as given in Figure 23 were taken. In obtaining this data the gas flow was studied with the cell at room temperature. The d-c heater power was applied and on reaching 850°C measurements were started. The voltage drift is nearly linear with time for 24 minutes. The magnitude of the voltage drift during this time is 0.6 mv and would represent a small change in the measured oxygen concentration. However, more disturbing is the shift of some 4 mv between Figure 23 and Figure 21. The cause of such shifts is not completely understood. Possible causes could be minute gas leaks, electrical leakage between the heater and cell, and minute fuel contamination in the system.

The overall response of the miniature cell to changes in oxygen concentration is illustrated in Figure 24. A major part of the response time observed is due to sweeping the original mixture out of the volume represented by the flowmeter and tubulation leading to the oxygen gauge. In taking the four curves the

voltage sensitivity of the scope was 2 mv/cm (1 div) and the sweep was 5 sec/cm. A flow rate of .06 SCFH was used for all gases and the reference gas was 40% oxygen. In Curve A, 13.2% was switched to 19.7% at the start of the trace. In each case the original trace is continued with a second trace. Curve B corresponds to switches from 13.2% oxygen to 26.4% oxygen. Curve C corresponds to switching from 19.7% oxygen to 13.2% oxygen. Curve D corresponds to switching from 26.4% oxygen to 13.2% oxygen. The system reaches 90-95% of the true value within 60 seconds. The time lag is due primarily to the sweeping of the volumes external to the cell.

In search of the cause of voltage differences, curves of the type shown in Figures 25 and 26 were taken. In taking these curves the heater was turned on with the cell at room temperature. 1 on the curve corresponds to the first measurement on reaching 850°C. Each succeeding point is separated in time by three (3) minutes. Immediately after each measurement the gas flow was changed and at the end of the 3-minute interval the next voltage measurement was taken. In general, the drift of the type shown in Figure 23 is observed. Cycling of the flow in this manner shows that the magnitude of the voltage change associated with flow changes of .02-.08 SCFH in one bore while maintaining the reference at .06 SCFH is of the order of 0.5 mv. The large change in voltage output in switching the reference and sample gas (6 mv) was found later to be largely associated with a leak in a seal. Closing of this reduced the voltage change on reversing the gas stream from one bore (L) to the other (R) to 2-3 mv. The cause for this change is not understood and will require further investigation.

The power requirements of the sensor is approximately 14 watts at 25 volts d-c. A small fraction of this power is required in heating the gas required for operation. The influence on the cooling rate of the cell by the gas

is shown in Figure 27. At time zero the heater power was switched off and gas flow maintained. The differences in the cooling rates for the three conditions are small as measured on the thermocouples. Additional investigation directed toward optimizing the insulation surrounding the heater could result in lowering the power requirements of the sensor.

Figure 28 is a calibration flow rate curve for the plastic capillaries used in the miniaturized oxygen sensor system shown in Figure 10.

In Figure 29 is shown the experimental error band for the oxygen flight sensor in the pressure range of 100-200 mm Hg. The sensor is useful in the measurement of oxygen pressure over a much larger pressure range than that shown in Figure 29.

The design objectives as described in the contract work statement have all been achieved. However, insufficient time was available to optimize some of the parameters which, therefore, were determined empirically.

In order for the signal to be linear within 1% over the range of 100-200 mm Hg oxygen pressure of test gas, a reference gas with an oxygen partial pressure of the order of 1 mm Hg should be provided. This could be accomplished by using a special reference gas of low oxygen partial pressure, which could be exhausted within the vehicle, or by utilizing the vacuum external to the capsule and dumping pure oxygen reference gas overboard. Neither of these approaches seems to justify the 1% linearity requirement when all factors are considered.

If a reference gas of pure oxygen at a pressure slightly above capsule ambient can be used, both the reference and test gases can be exhausted to the ambient without waste. In this case the deviation from linearity in the range of 100-200 mm Hg oxygen pressure would be of the order of 5%.

The complete sensor weighs approximately fifty (50) grams, occupies a volume of 18cc, and operates at 850°C using approximately 14 watts of d-c power. Flow rates of the two gases are in the range of .06 SCFH at atmospheric pressures. Charging the sensor at the rate of 0.3 pounds per watt of power used and assuming the reference and test gases are exhausted within the capsule, the total weight chargeable to the sensor is approximately 4.32 pounds. Only about 3% of this is actual sensor weight, with 97% charged for power. It appears that some trade-off between sensor weight and power required would permit a considerable savings in total weight chargeable to the sensor. However, consideration of the quantity of reference gas used must be made if it is necessary to dump it overboard. At the flow rate mentioned above about 16 pounds of oxygen would be used in 100 days, although lower flow rates can be used as total pressure of capsule ambient decreases below atmospheric pressure.

The sensor is capable of monitoring oxygen partial pressures over a much larger range than the 100-200 mm Hg range of interest specified. Broad latitude in the selection of reference gas conditions is possible such that almost any desired range of oxygen pressure can be monitored.

The response time of the sensor itself is of the order of milliseconds. Plumbing lines for the gases should be kept to as small a volume as practicable in order that gas transport times, which cause the major delay in response, will not be excessive.

The shelf life of the sensor, although not specifically determined, is fully expected to exceed one (1) year and could reasonably be expected to exceed five (5) years.

## ACKNOWLEDGMENTS

The assistance of the following Westinghouse personnel is also hereby acknowledged:

W. G. Carlson - Supervising Engineer, Ceramics Dept., Research and Development Center

C. J. Cassidy - Supervisor, Glassblowing Department, Research and Development Center

C. C. Glover - Engineering Manager, Scientific Equipment Department

T. G. Spofford - Engineer, Scientific Equipment Dept.

## TABLE OF FIGURES

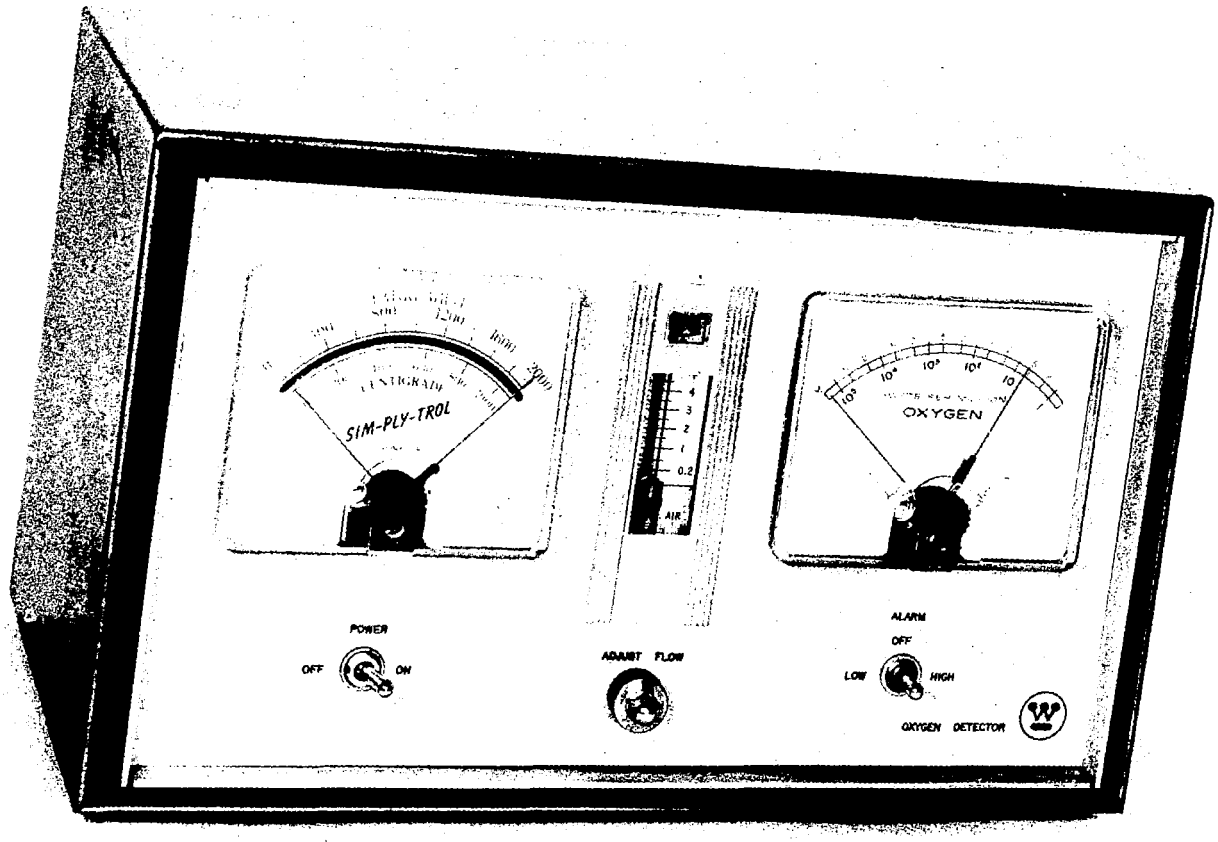


Fig. 1—Westinghouse solid electrolyte oxygen gauge

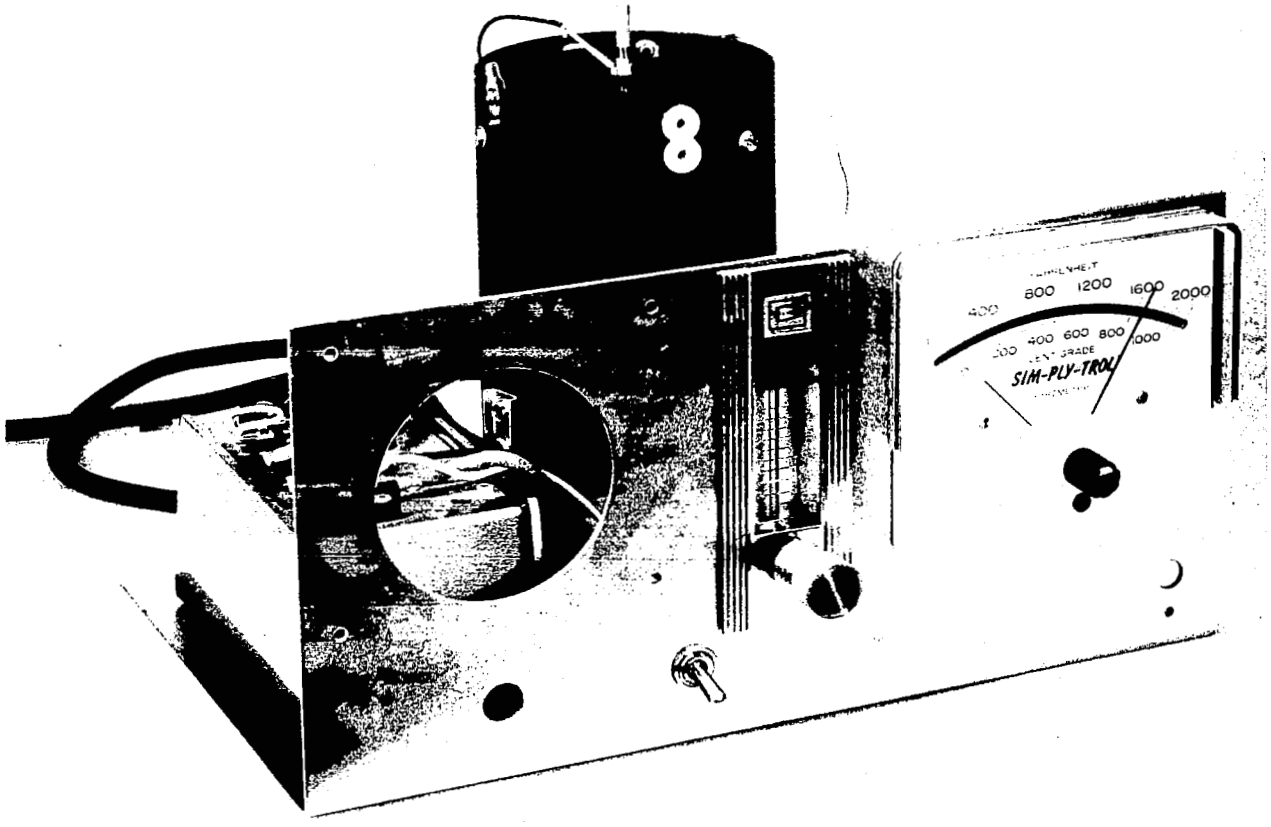


Fig. 2—Test setup for standard size oxygen sensor

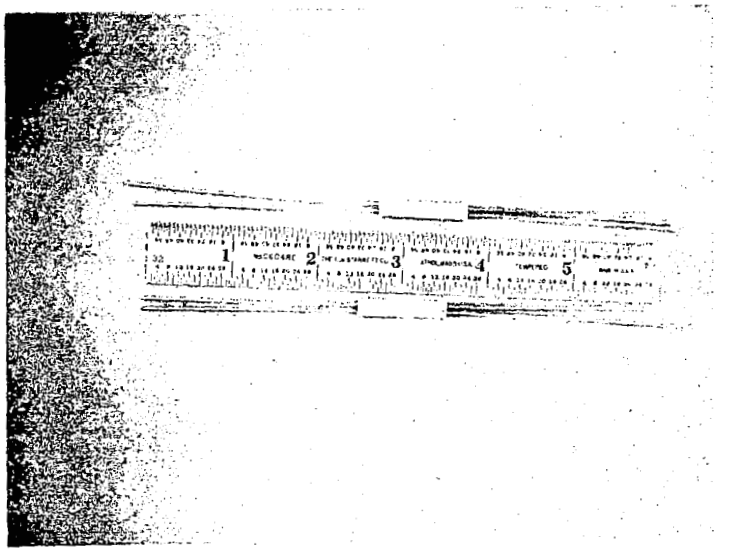

Fig. 3— Assembled oxygen sensors

Fig. 4—End view of sensor showing hermetic seal of tubular platinum leads to solid electrolyte

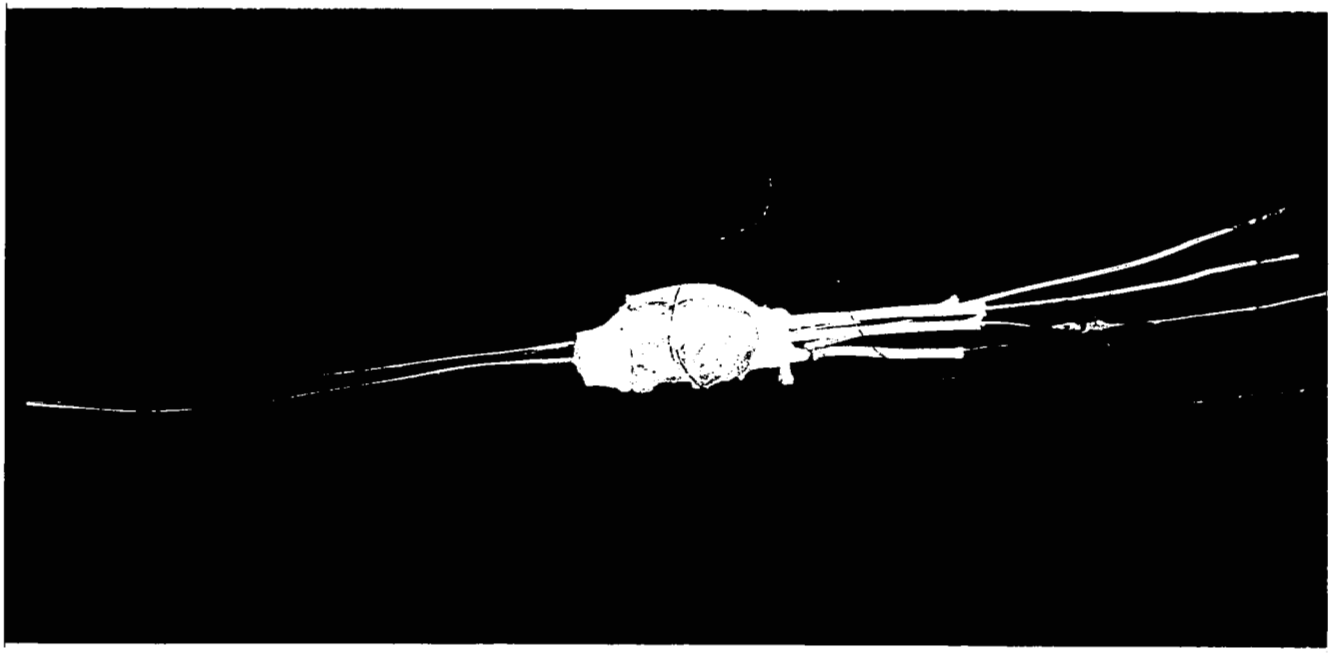

Fig. 5—Unmounted miniature sensor

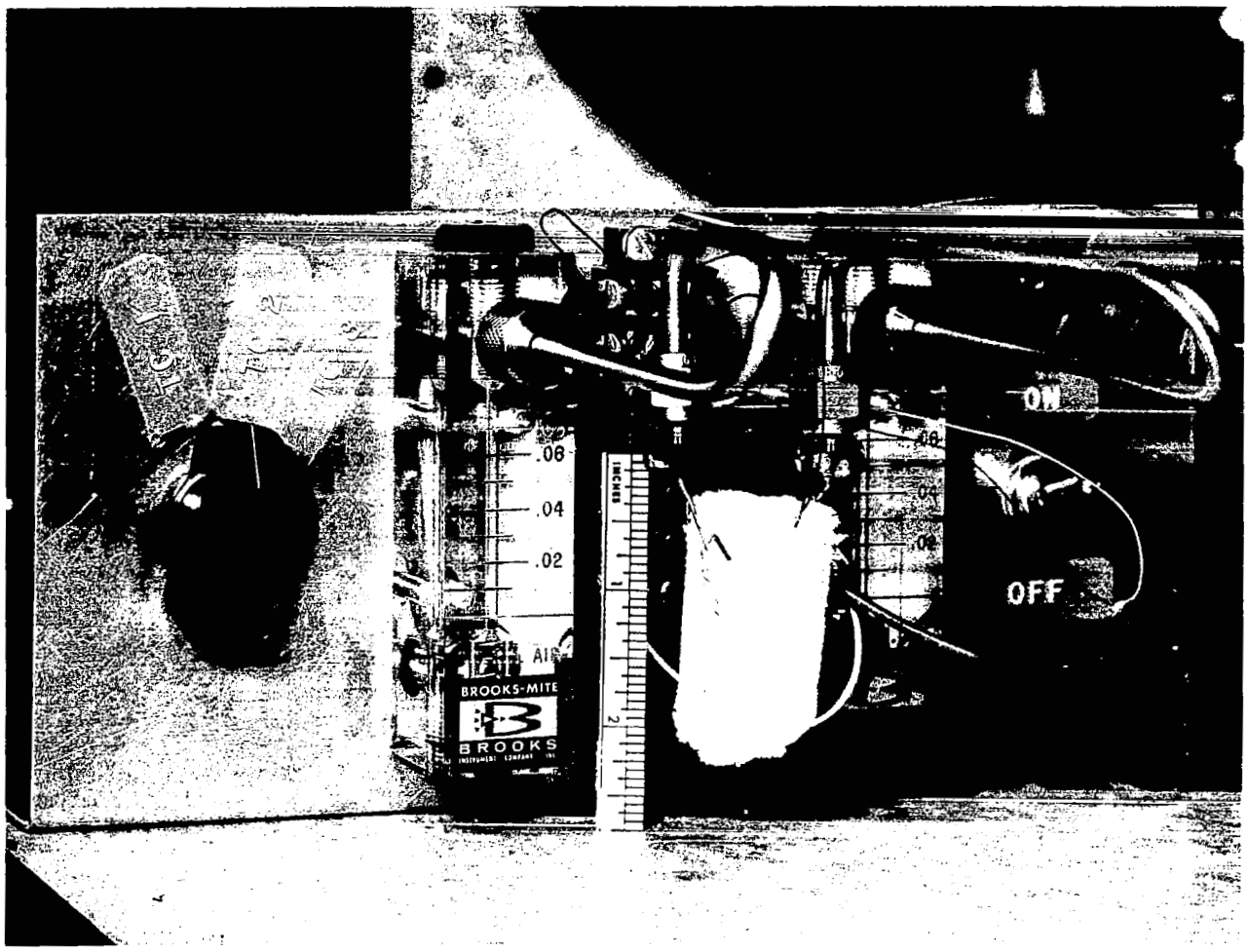


Fig. 6—Prototype miniature sensor system

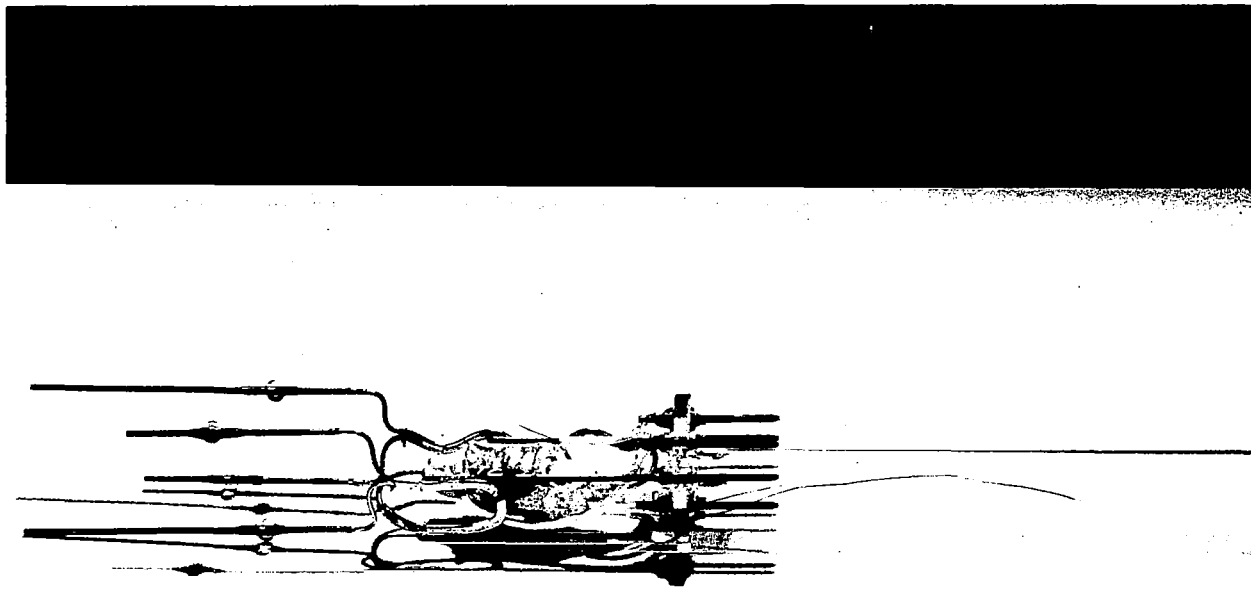

Fig. 7—Miniature sensor mounted on press

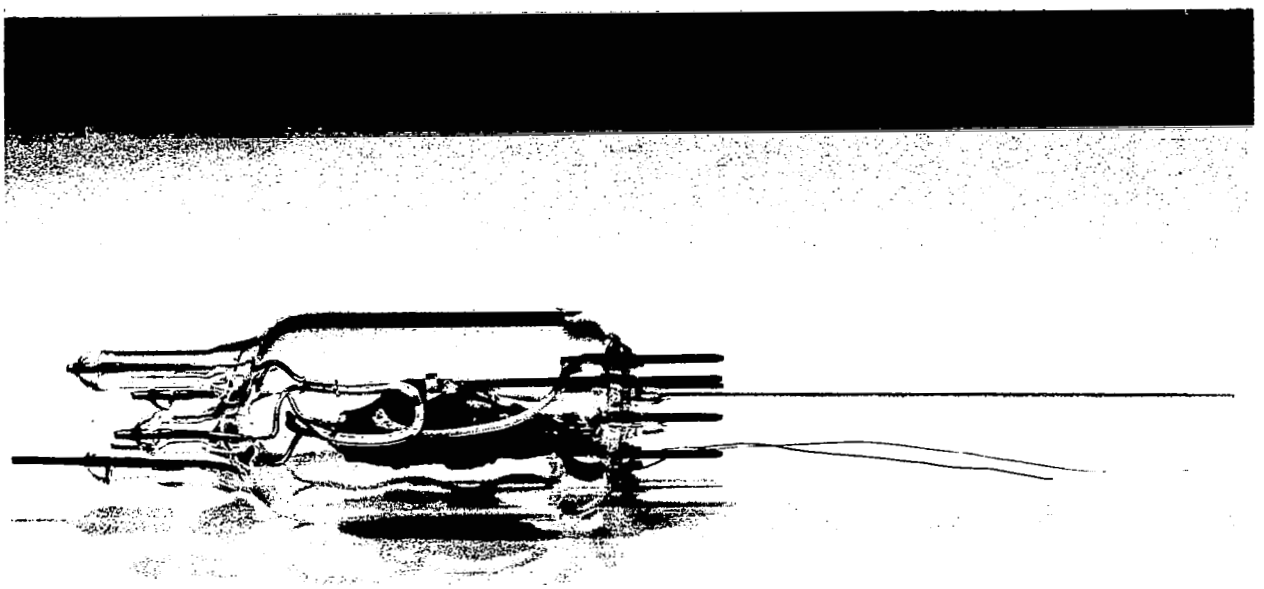

Fig. 8—Glass encapsulated miniature sensor


Fig. 9—Completed miniature oxygen sensor

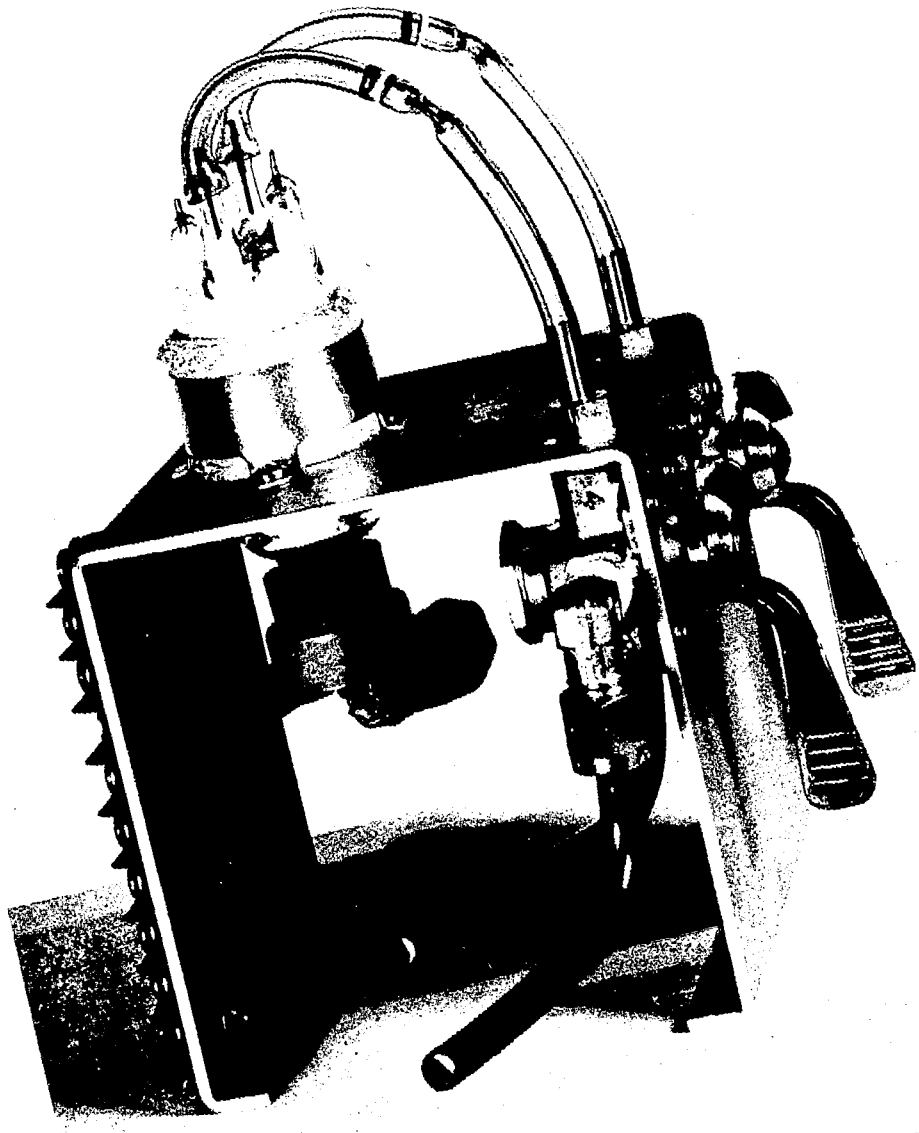

Fig. 10—Miniaturized oxygen sensor system

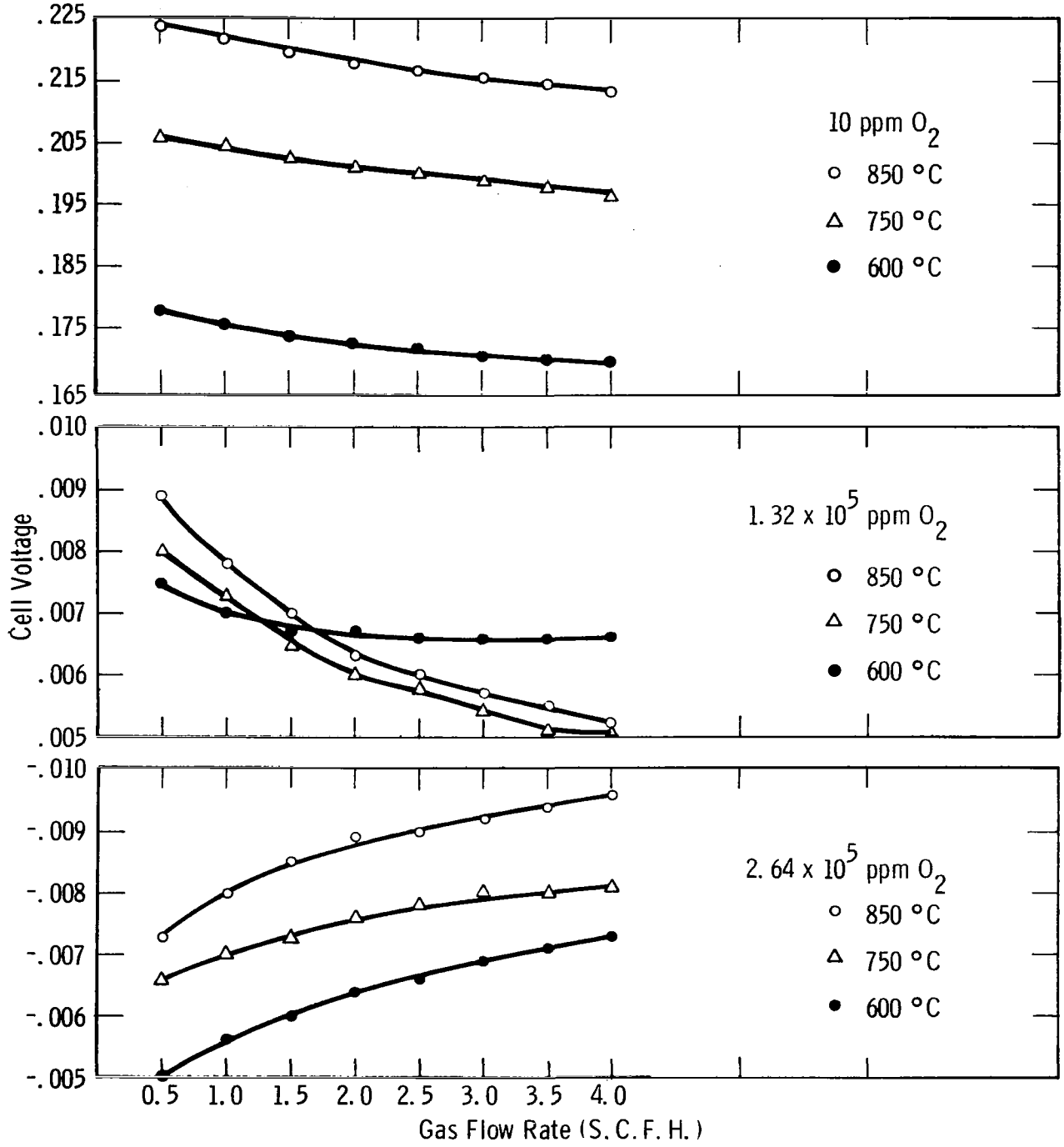


Fig. 11— Voltage vs gas flow rate for standard cell

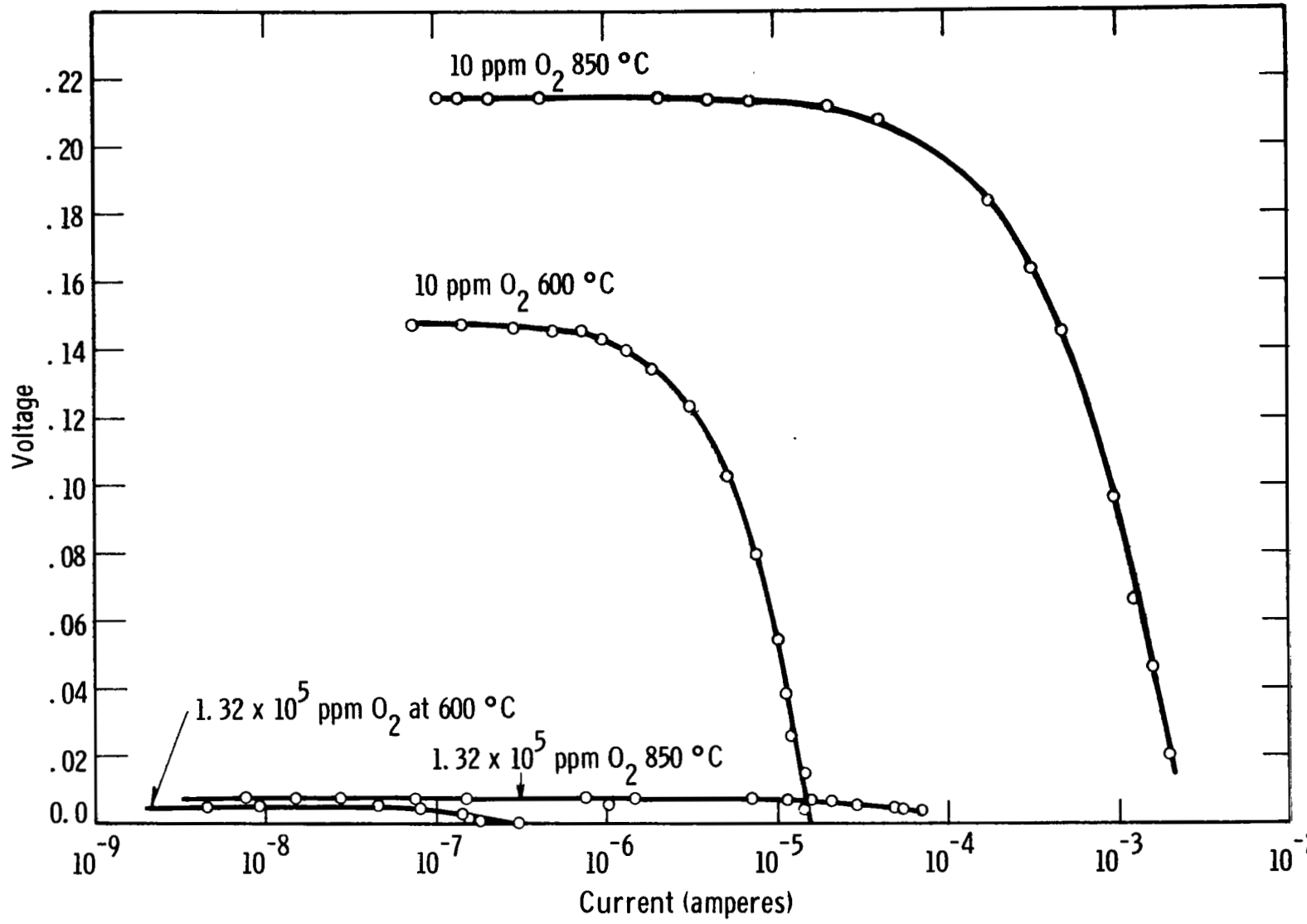


Fig. 12— Voltage vs current for standard cell

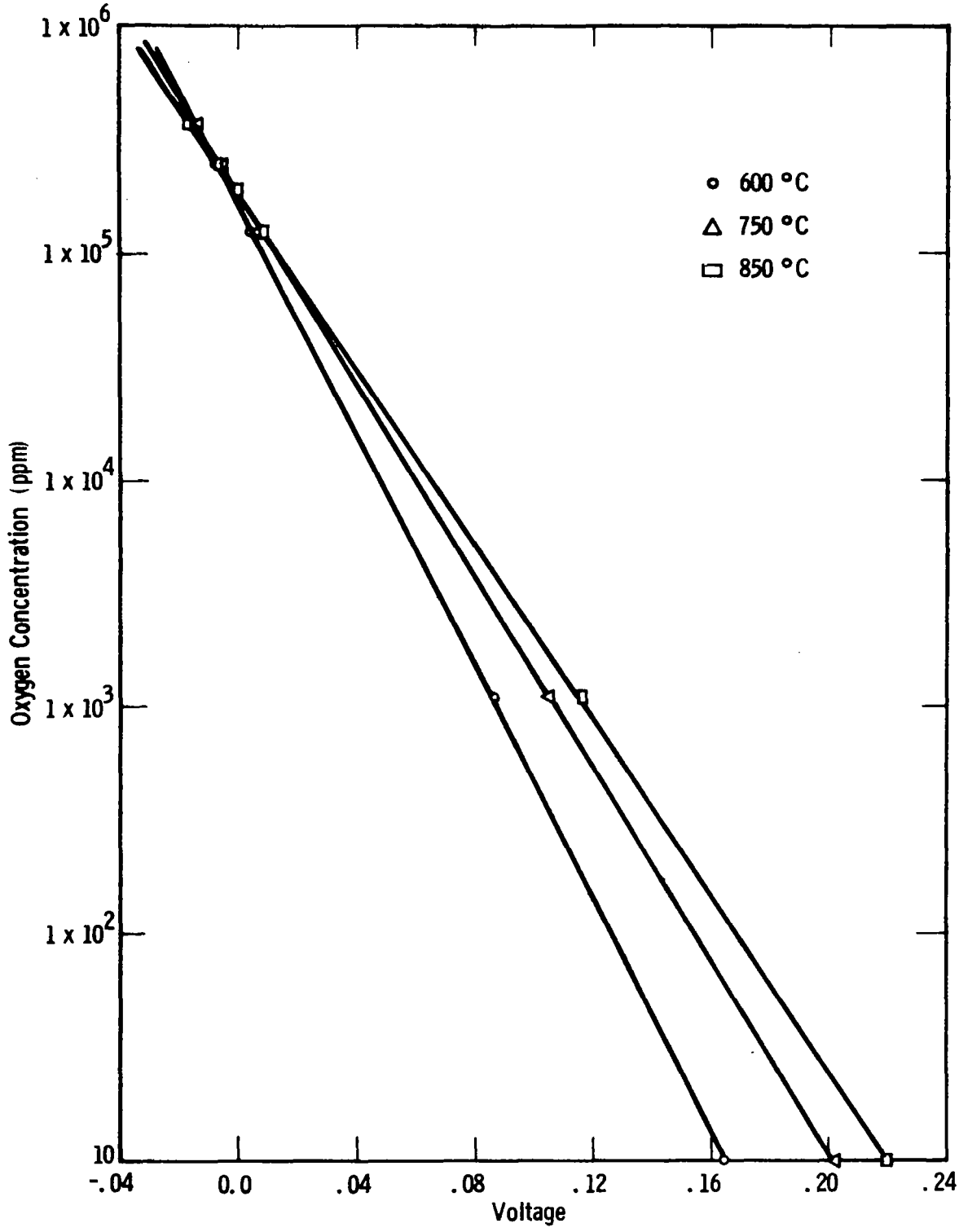


Fig. 13— Oxygen contentration vs voltage for standard cell

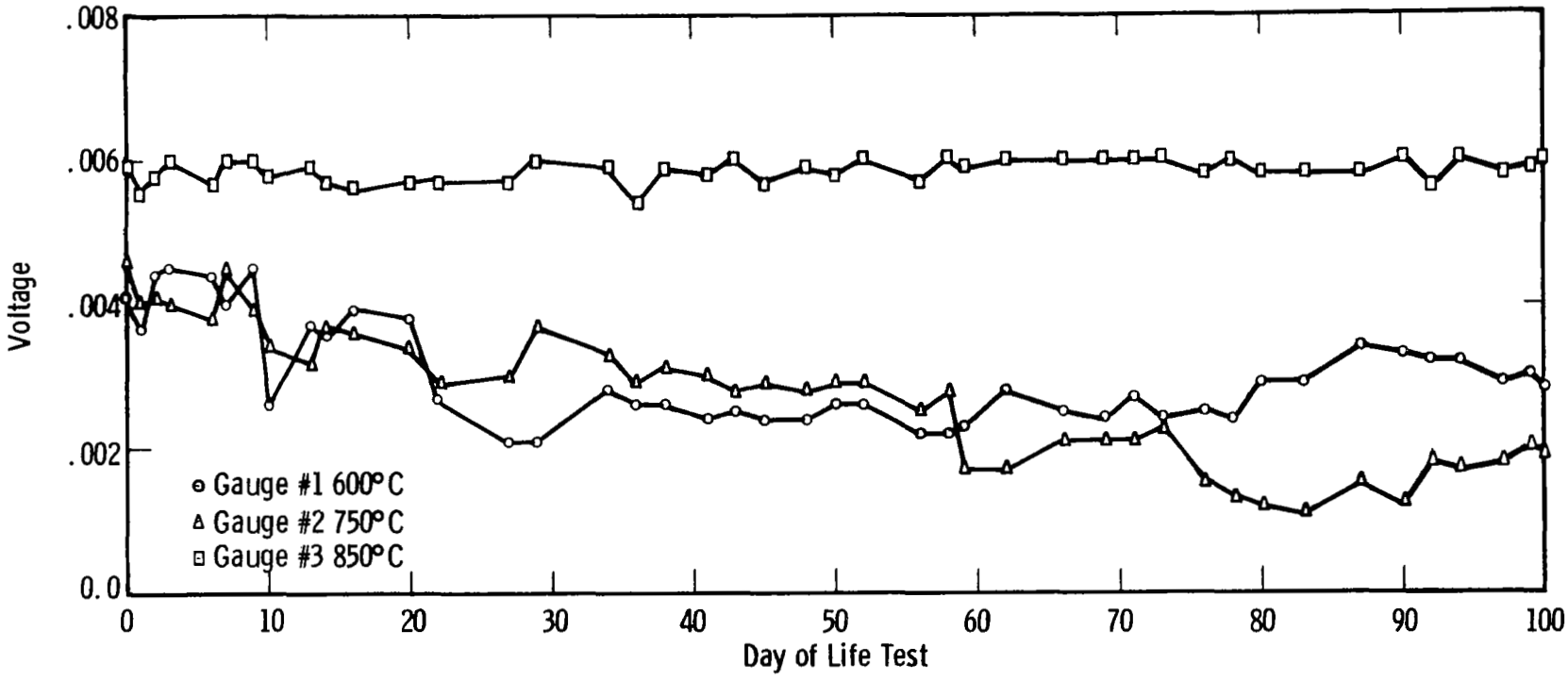


Fig. 14— Life test on oxygen gauge ( 100 mm Hg $O_2$ pressure in $N_2$)

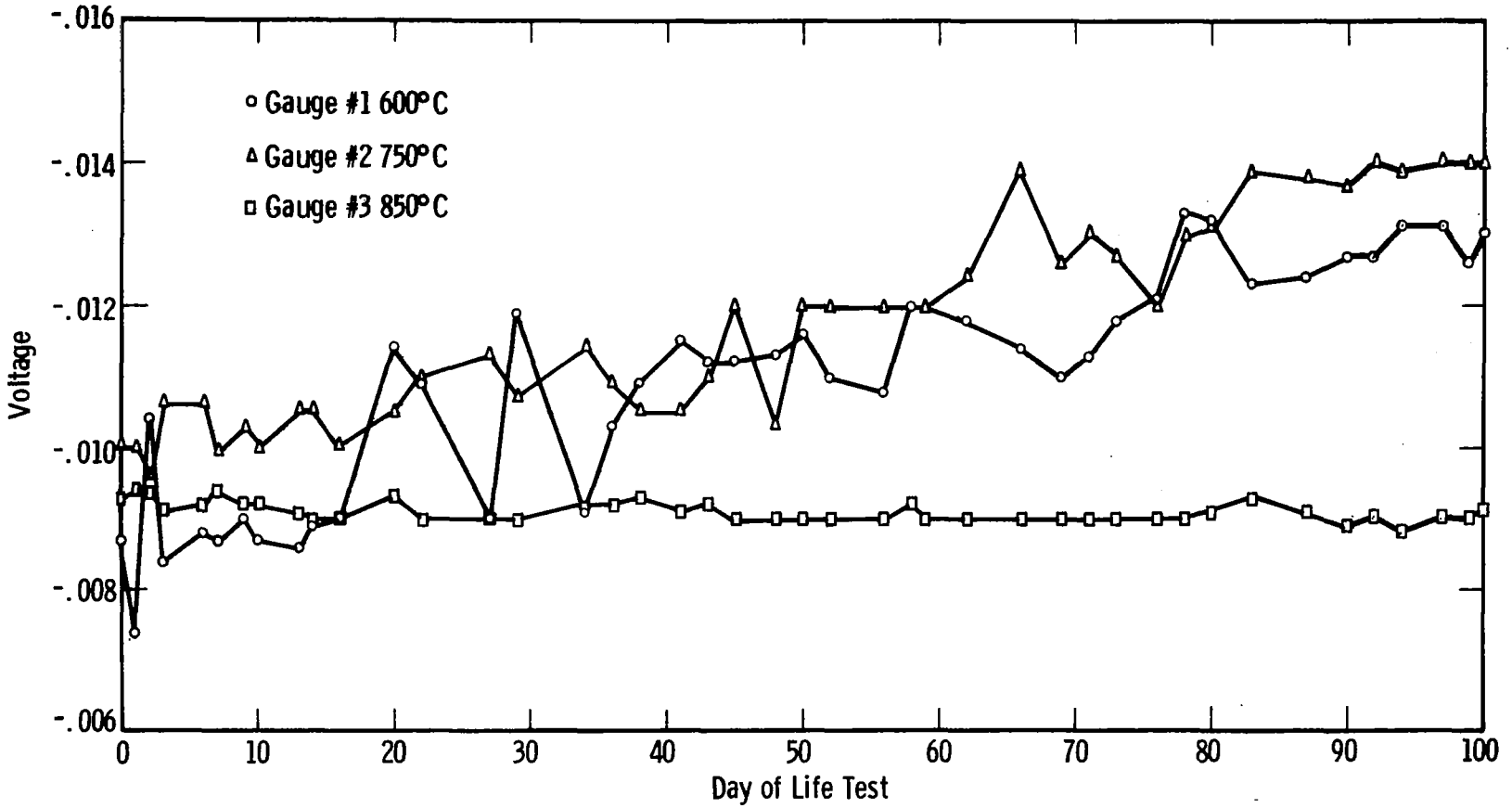


Fig. 15— Life test on oxygen gauge (200 mm Hg $O_2$ pressure in $N_2$)

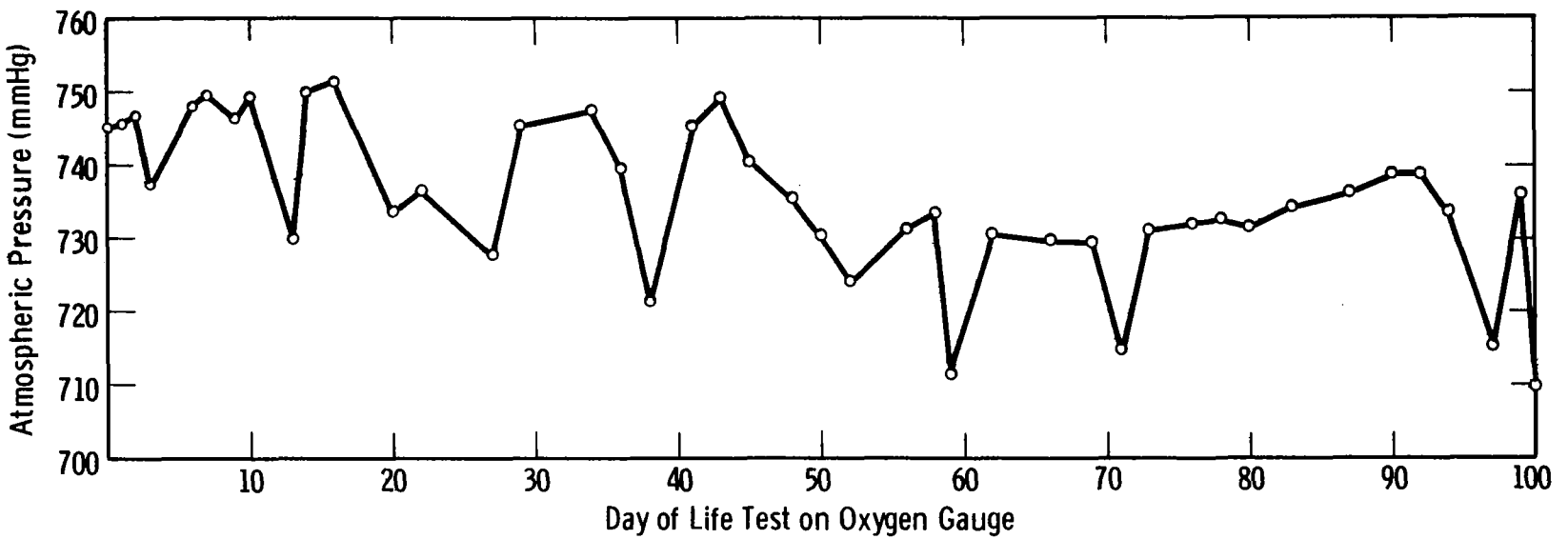


Fig. 16—Atmospheric pressure during life test

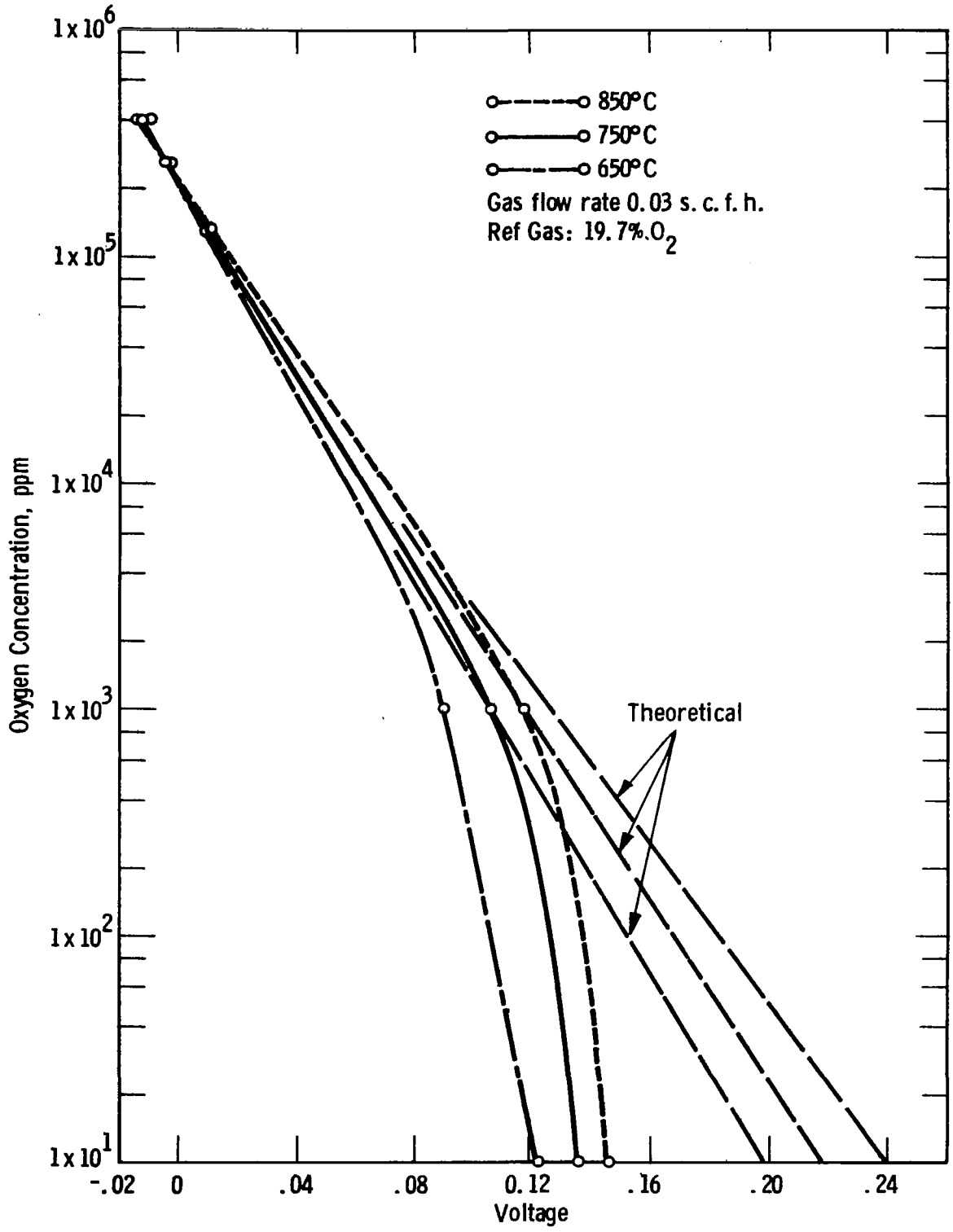


Fig. 17 —Oxygen concentration vs voltage curves at 650°C, 750°C, and 850°C for 6" long small cell

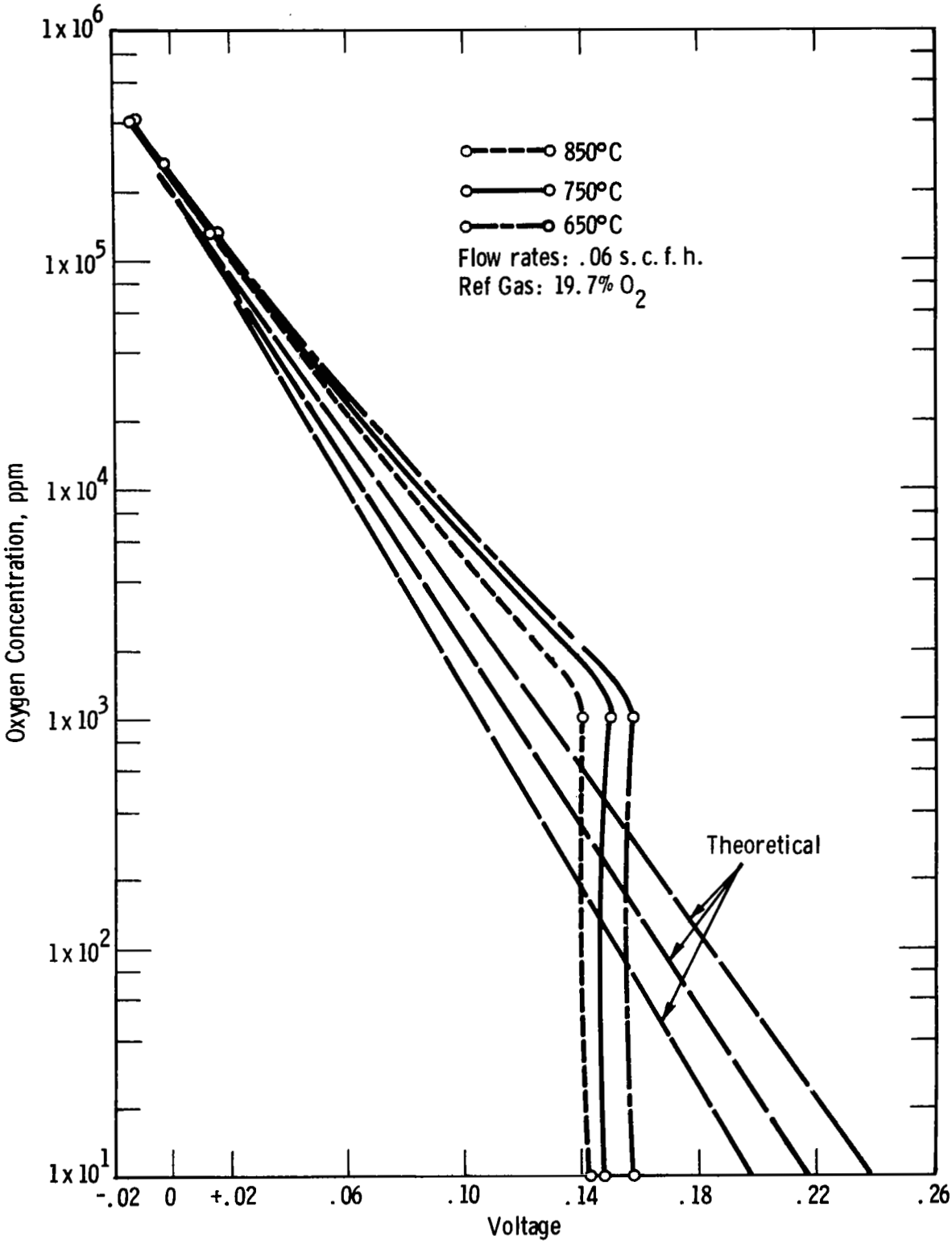


Fig. 18 —Oxygen concentration vs voltage curves at 650°C, 750°C, and 850°C for small cell

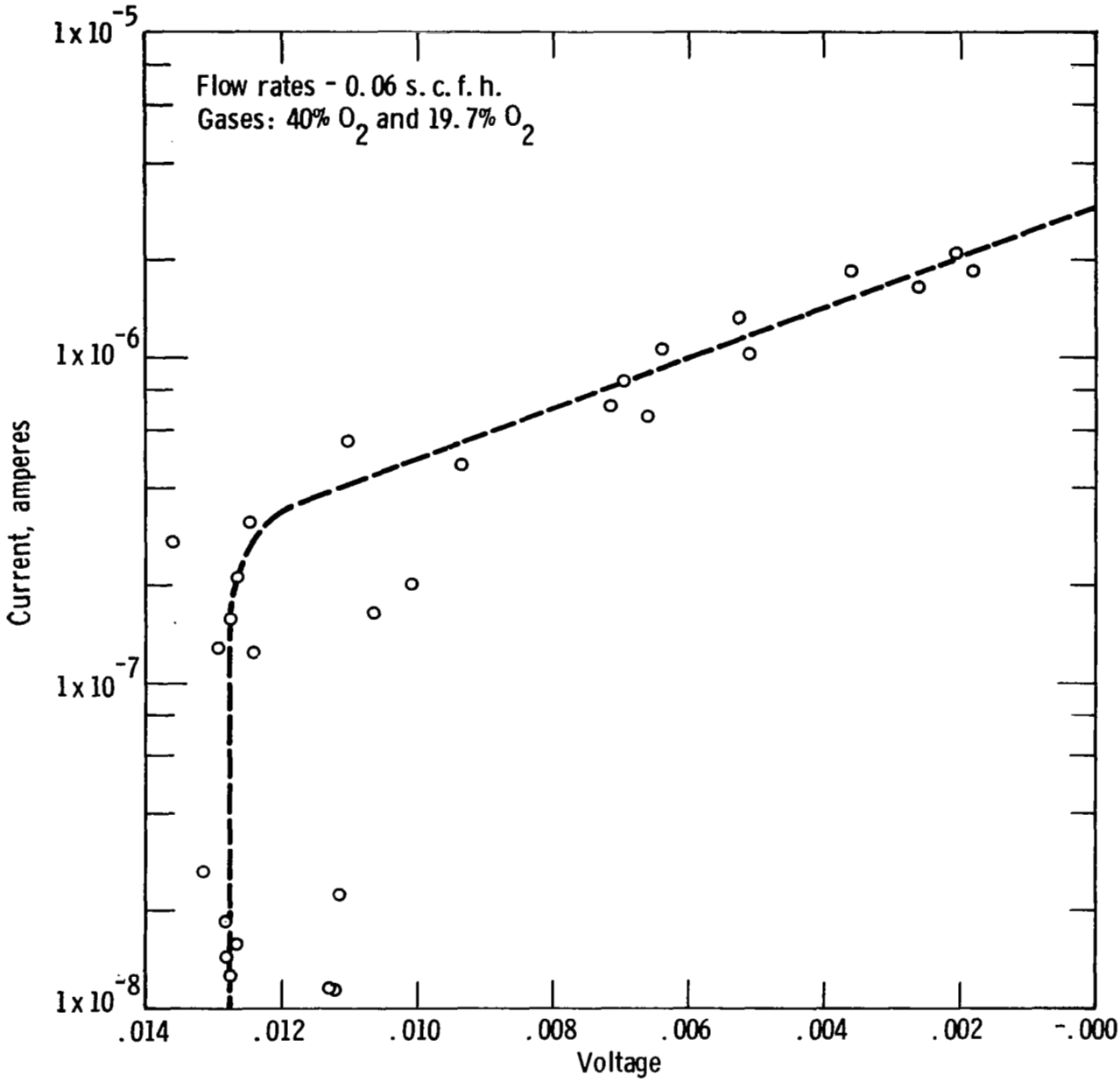


Fig. 19 —Current vs voltage curve for small cell at 850°C

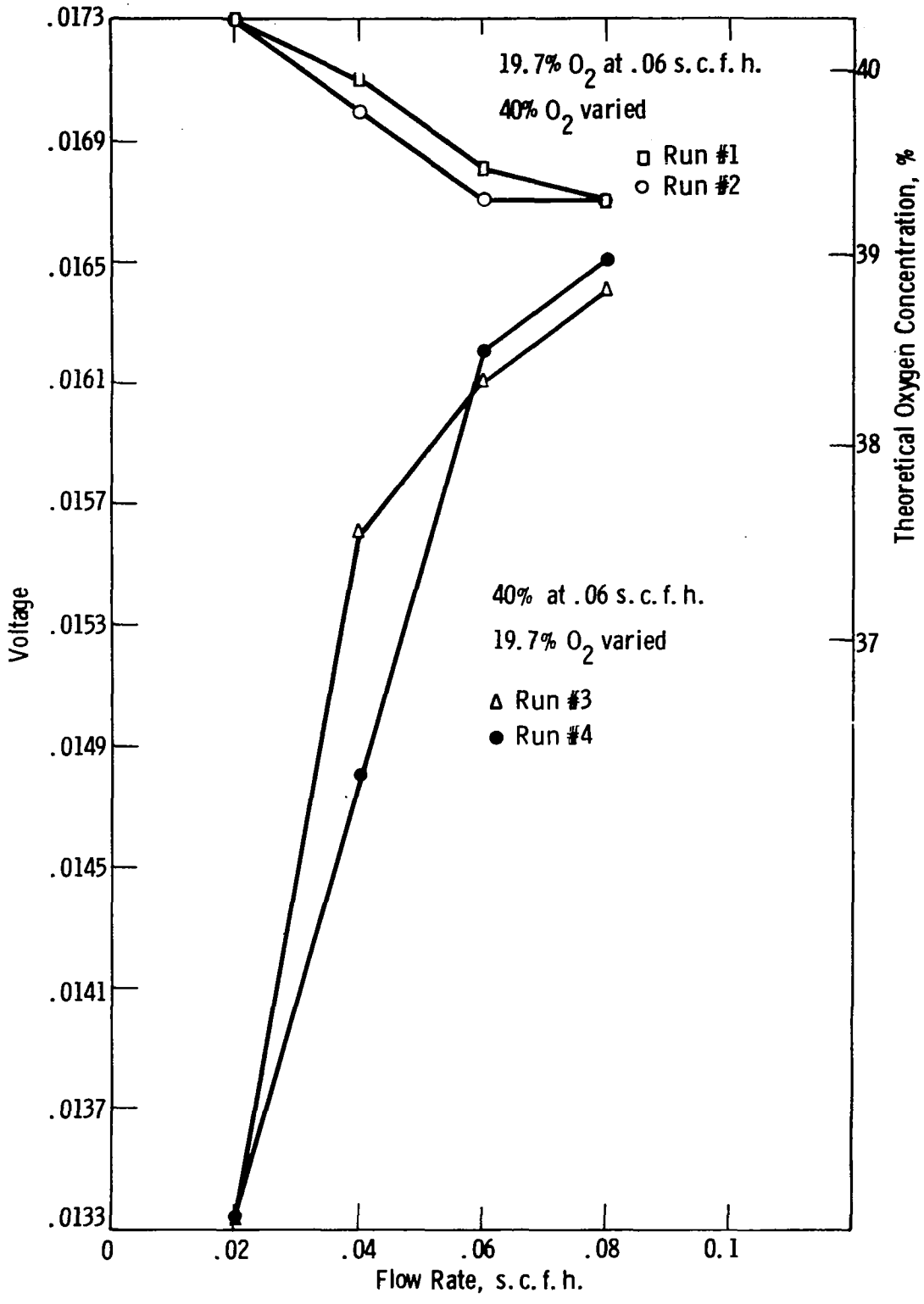


Fig. 20 —Voltage vs flow rate curves for small cell

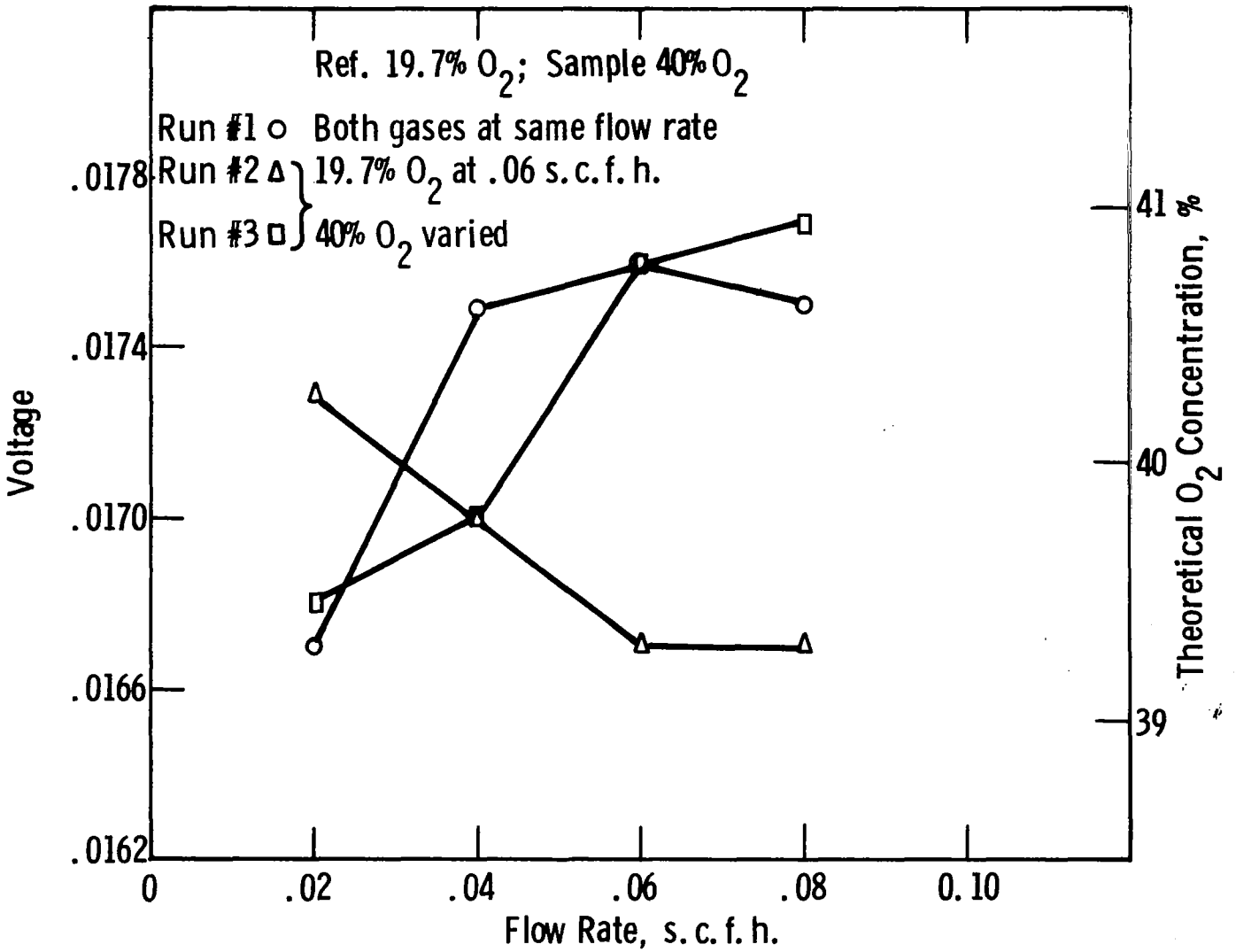


Fig. 21 —Voltage vs flow rate for small cell

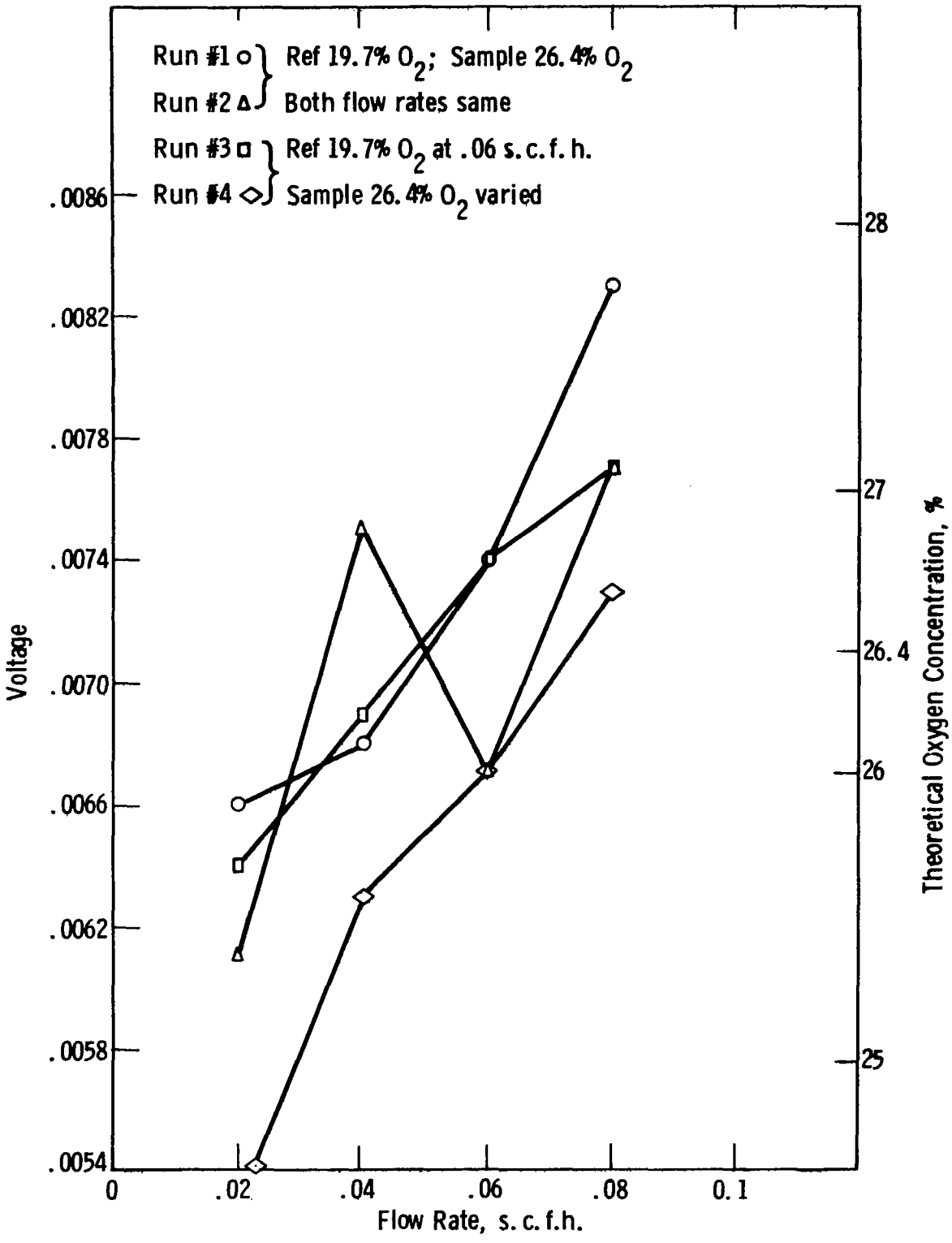


Fig. 22—Voltage vs flow rate for small cell

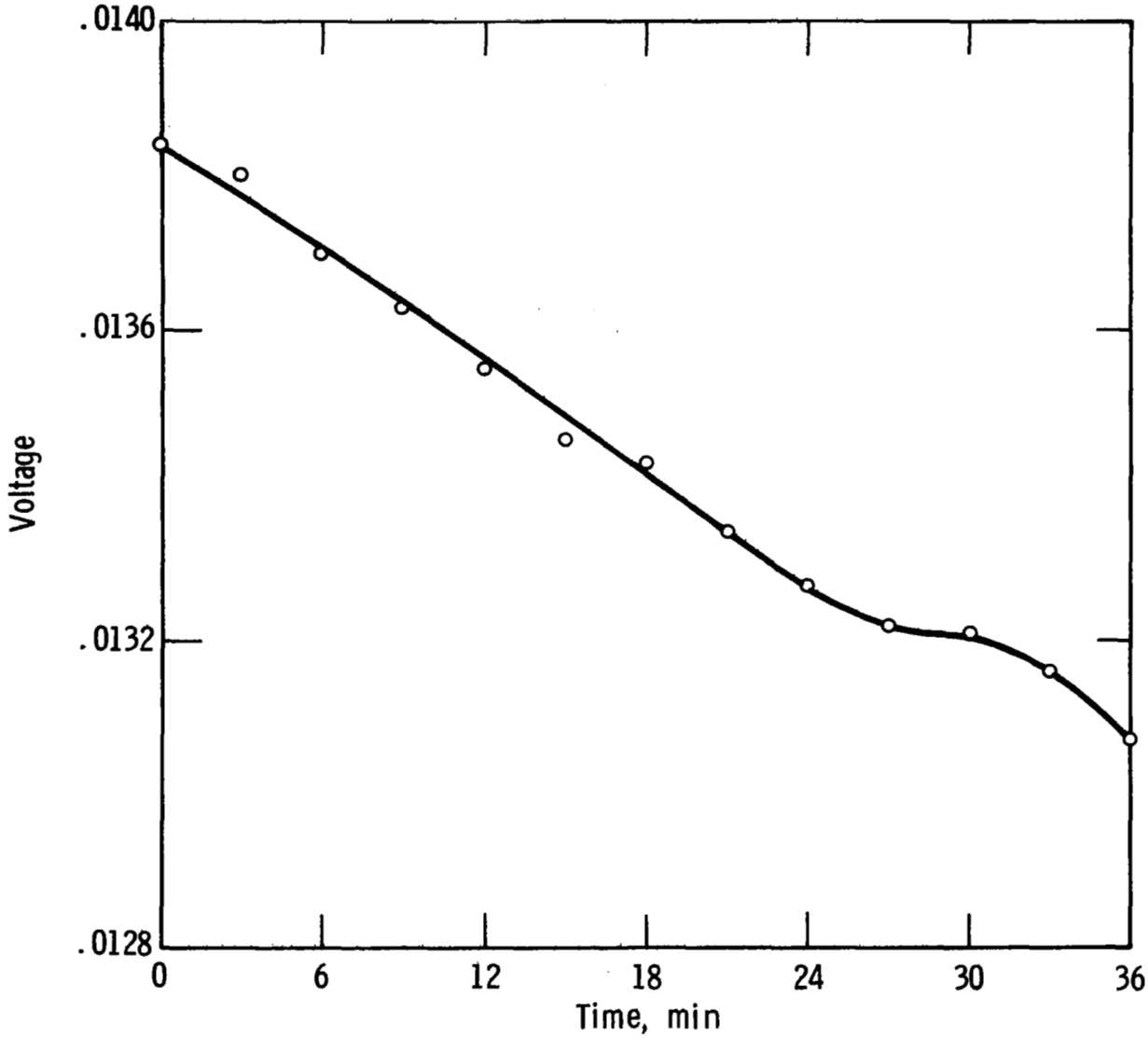


Fig. 23 —Cell voltage vs time using 19.7% and 40% oxygen at .06 S.C.F.H. flow rate

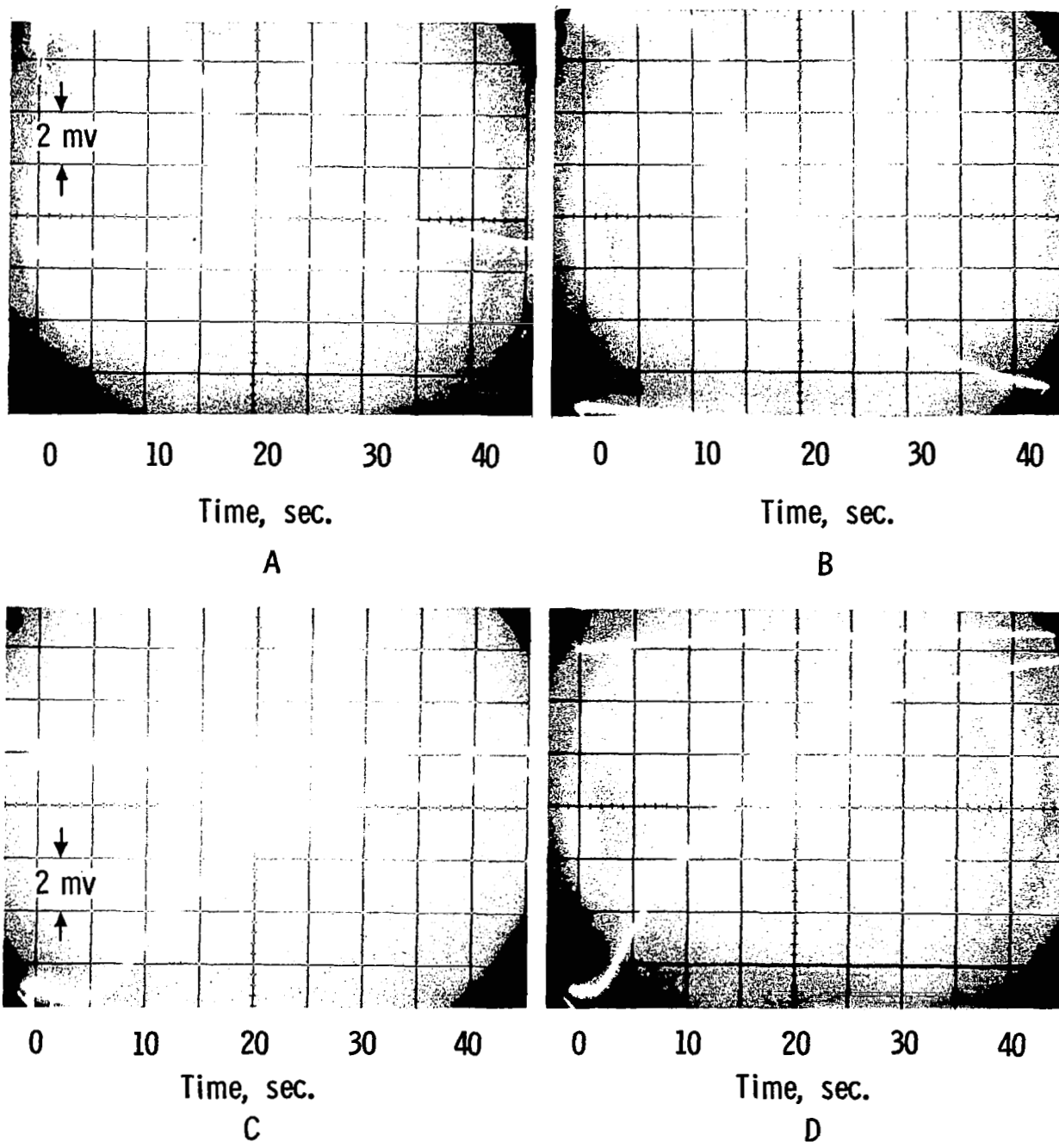


Fig. 24 —Oscillographic traces of output voltage vs time in response to change in gas composition

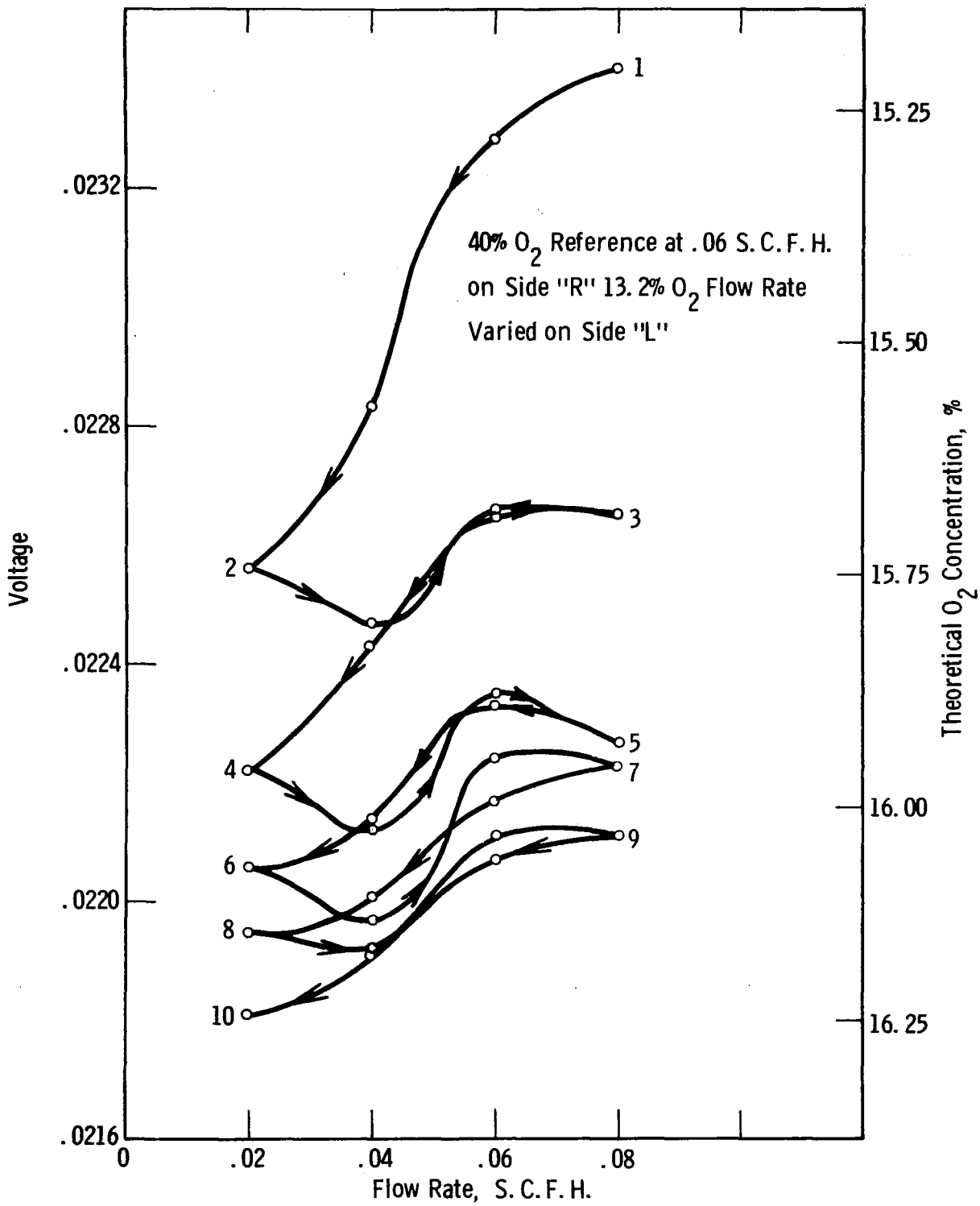


Fig. 25 —Cell voltage during cycling of flow rate over elapsed time of two hours

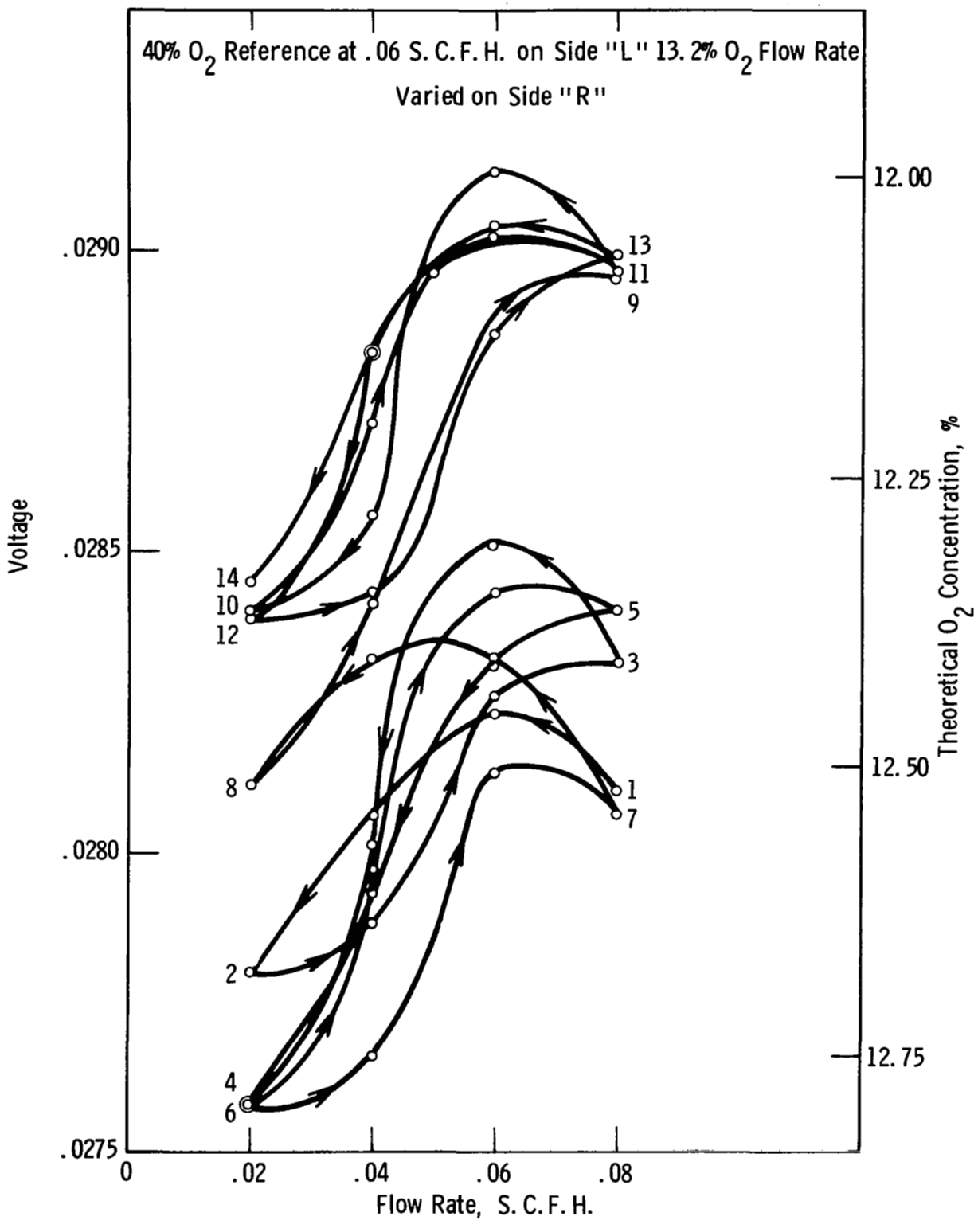


Fig. 26—Cell voltage during cycling of flow rate over elaspsed time of two hours

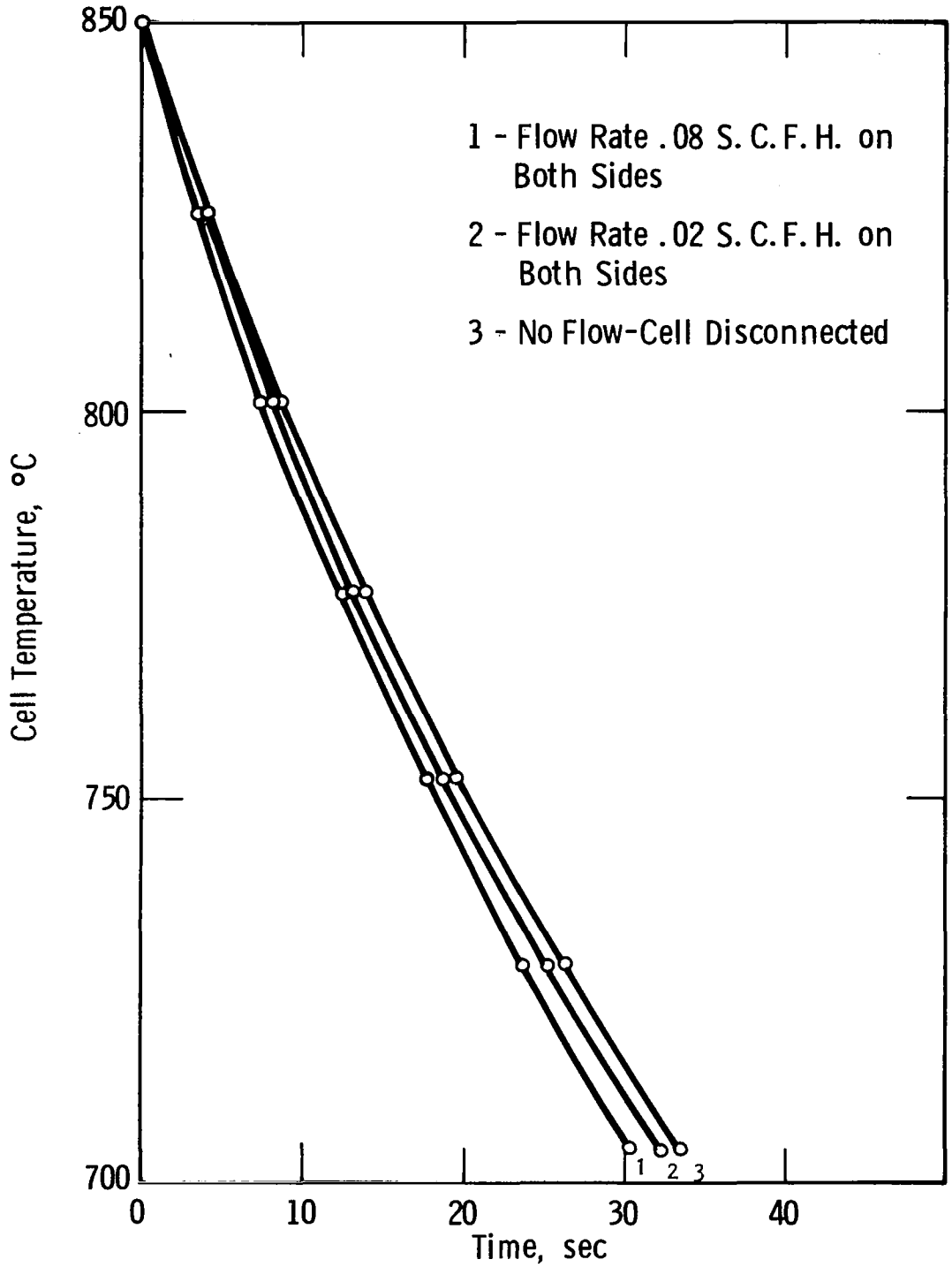


Fig. 27—Cooling curves for various flow conditions at zero furnace power

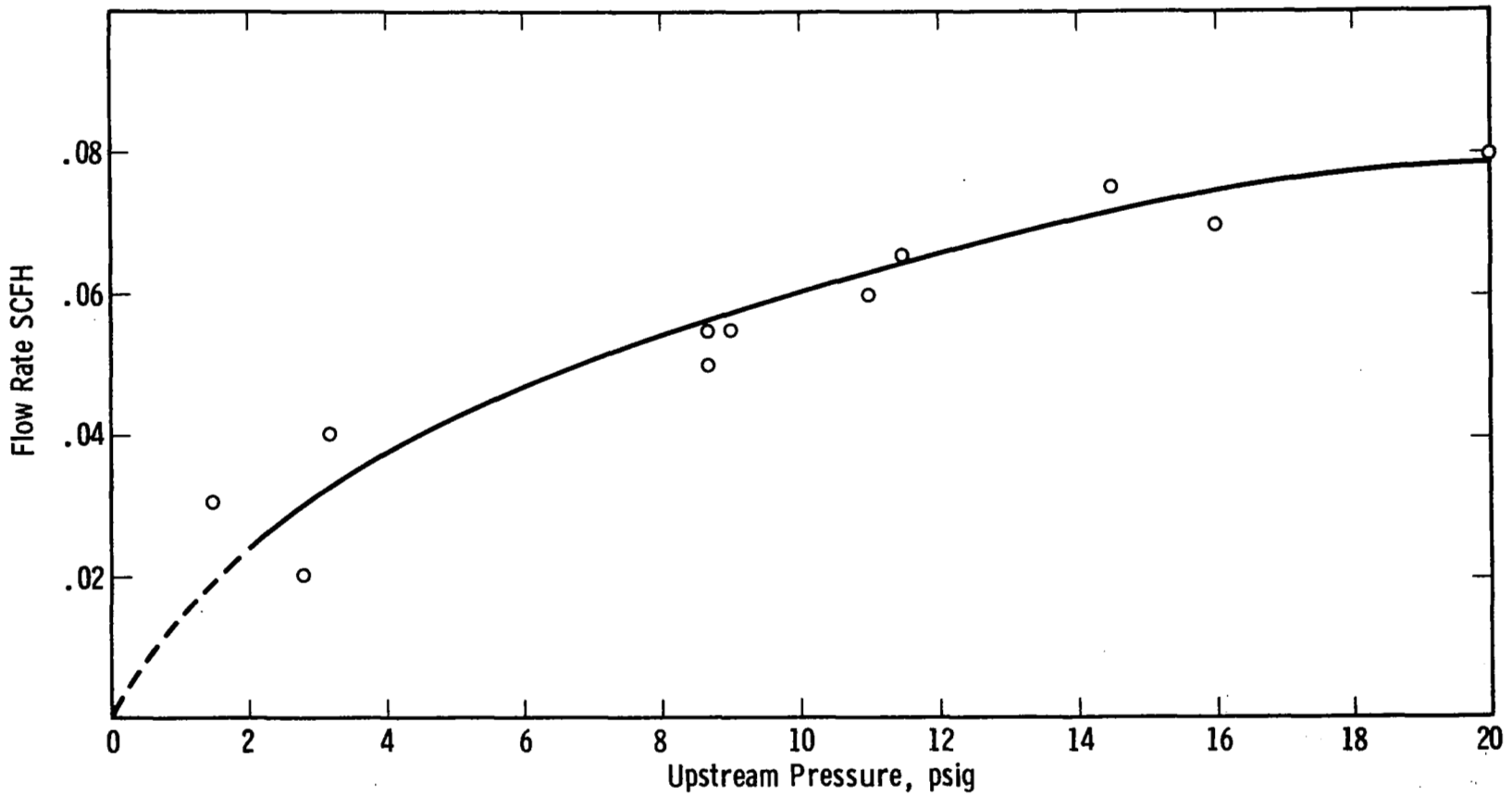


Fig. 28—Flow rate through plastic capillaries

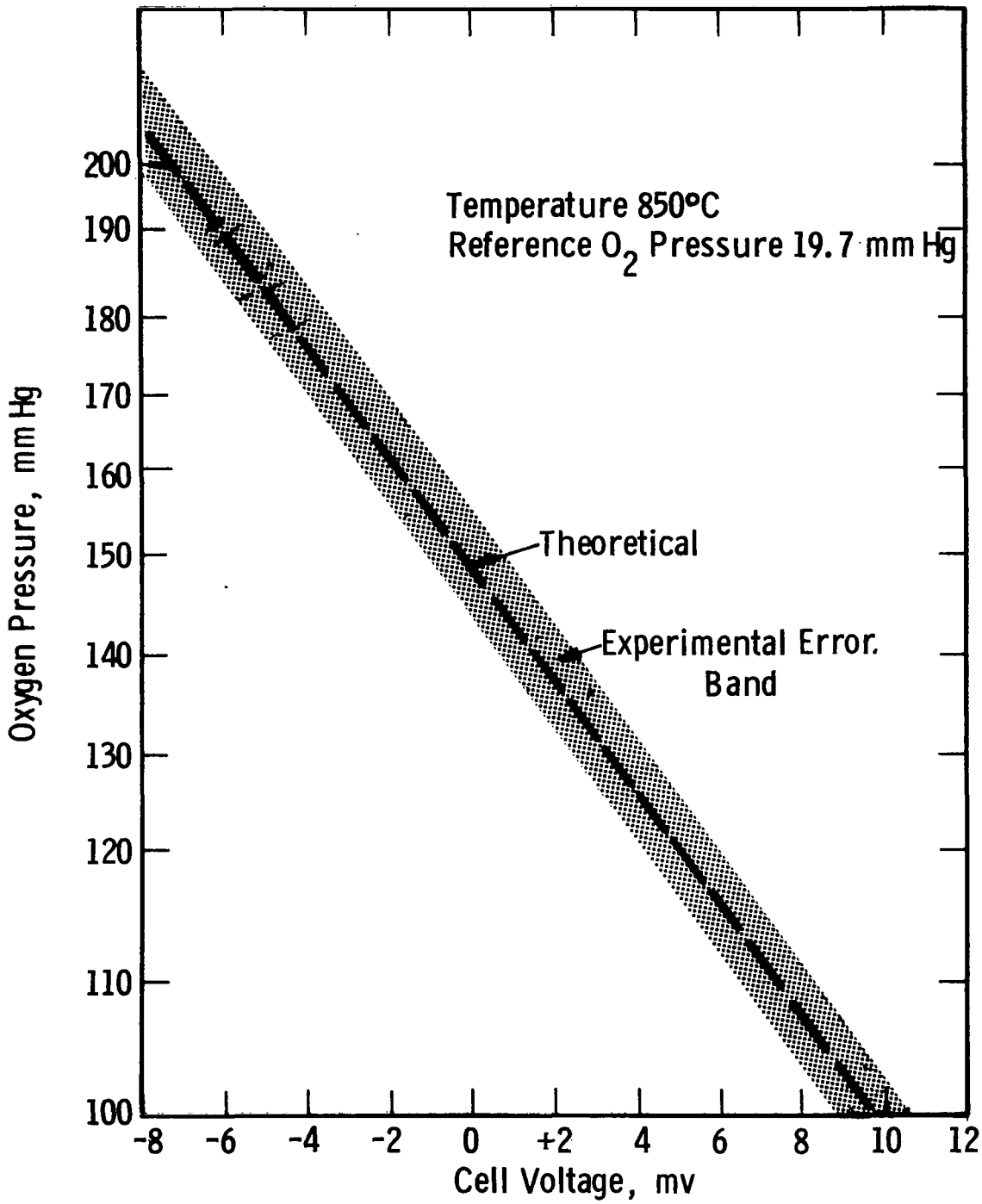


Fig. 29—Experimental error band for oxygen flight sensor in the oxygen pressure range of 100-200 mm Hg